

**Towards a low-cost,  
non-invasive system for  
occupancy detection using  
a thermal detector array**

Ash Tyndall

*This report is submitted as partial fulfilment  
of the requirements for the Honours Programme of the  
School of Computer Science and Software Engineering,  
The University of Western Australia,  
2015*

# Abstract

This is the abstract.

**Keywords:** keyword, keyword

**CR Categories:** category, category



© 2014–15 Ashley Ben Tyndall

This document is released under a Creative Commons Attribution-ShareAlike 4.0 International License. A copy of this license can be found at <http://creativecommons.org/licenses/by-sa/4.0/>.

A digital copy of this document and supporting files can be found at <http://github.com/atyndall/honours>.

The following text can be used to satisfy attribution requirements:

“This work is based on the honours research project of Ash Tyndall, developed with the help of the School of Computer Science and Software Engineering at The University of Western Australia. A copy of this project can be found at <http://github.com/atyndall/honours>.<sup>”</sup>

Code and code excerpts included in this document are instead released under the GNU General Public License v3, and can be found in their entirety at <https://github.com/atyndall/thing>.

# Acknowledgements

These are the acknowledgements.

# Contents

<b>Abstract</b>	<b>ii</b>
<b>Acknowledgements</b>	<b>iv</b>
<b>1 Introduction</b>	<b>1</b>
<b>2 Literature Review</b>	<b>3</b>
2.1 Intrinsic traits . . . . .	4
2.1.1 Static traits . . . . .	4
2.1.2 Dynamic traits . . . . .	6
2.2 Extrinsic traits . . . . .	6
2.2.1 Instrumented traits . . . . .	6
2.2.2 Correlative traits . . . . .	7
2.3 Analysis . . . . .	8
2.4 Thermosense . . . . .	10
2.4.1 Classification Algorithms . . . . .	10
2.4.1.1 Neural Networks . . . . .	11
2.4.1.2 k-nearest Neighbors . . . . .	12
2.4.1.3 Linear Regression . . . . .	13
2.4.1.4 Naive Bayes . . . . .	13
2.4.1.5 Support Vector Machines . . . . .	13
2.4.1.6 Decision Trees . . . . .	14
2.4.1.7 KStar . . . . .	14
2.4.1.8 0-R . . . . .	15
2.5 Research Gap . . . . .	15

<b>3 Design and Implementation</b>	<b>16</b>
3.1 Hardware . . . . .	16
3.1.1 Sensing . . . . .	17
3.1.2 Pre-Processing . . . . .	19
3.1.3 Analysis / Classification . . . . .	19
3.1.4 Component Costs . . . . .	20
3.2 Software . . . . .	20
3.2.1 Sensing . . . . .	21
3.2.2 Pre-Processing . . . . .	21
3.2.3 Analysis / Classification . . . . .	24
3.3 Conclusion . . . . .	26
<b>4 Evaluation</b>	<b>28</b>
4.1 Sensor Properties . . . . .	28
4.1.1 Bias . . . . .	28
4.1.2 Noise . . . . .	30
4.1.3 Sensitivity . . . . .	32
4.2 Energy Efficiency . . . . .	32
4.3 Classification Accuracy . . . . .	35
4.3.1 Data gathering . . . . .	35
4.3.2 Data labeling . . . . .	36
4.3.3 Feature extraction and data conversion . . . . .	36
4.3.4 Running Weka Tests . . . . .	37
4.3.5 Classifier Experiment Set 1 . . . . .	41
4.3.5.1 Individual sub-experiment results . . . . .	46
4.4 Thermosense Comparison and Discussion . . . . .	48
<b>5 Conclusions</b>	<b>50</b>
5.1 Accuracy . . . . .	50
5.2 Energy Efficiency . . . . .	50
5.3 Privacy . . . . .	51

5.4	Cost . . . . .	51
5.5	Future Directions . . . . .	51
5.5.1	Sub-pixel localization . . . . .	51
5.5.2	Improving Robustness . . . . .	51
5.5.3	Field-of-view modifications . . . . .	52
5.5.4	New Sensors . . . . .	52
5.6	Final Stuff . . . . .	52
	<b>Bibliography</b>	<b>52</b>
	<b>A Physical Form</b>	<b>56</b>
	<b>B Original Honours Proposal</b>	<b>58</b>
B.1	Background . . . . .	58
B.2	Aim . . . . .	59
B.3	Method . . . . .	60
B.3.1	Hardware . . . . .	60
B.3.2	Classification . . . . .	60
B.3.3	Robustness / API . . . . .	61
B.4	Timeline . . . . .	61
B.5	Software and Hardware Requirements . . . . .	62
B.6	Proposal References . . . . .	63

# List of Tables

2.1	Comparison of different sensors and project requirements . . . . .	8
3.1	Hardware tiers . . . . .	17
3.2	Our project component costs . . . . .	20
3.3	Thermosense component costs . . . . .	20
4.1	Weka parameters used for classifications . . . . .	38
4.2	Experiment Set 1 Script . . . . .	42
4.3	Classifier Experiment Set 1 Results . . . . .	45
4.4	Classifier Experiment Set 1 Individual Sub-experiment RMSEs . .	47

# List of Figures

2.1	Taxonomy of occupancy sensors . . . . .	4
3.1	MLX90620, PIR and Arduino integration circuit . . . . .	18
3.2	Prototype system architecture . . . . .	22
3.3	Initialisation sequence and thermal packet . . . . .	23
4.1	Experiment setup to determine sensor properties . . . . .	29
4.2	Plot of pixel means (top) and standard deviations (bottom) at rest	31
4.3	Noise levels of occupants (higher) and background (lower) at various sampling speeds . . . . .	33
4.4	Block diagram for the Melexis MLX90620 ( <i>Melexis</i> ) taken from datasheet [17] . . . . .	34
4.5	Different <i>Melexis</i> pixel temperature values as hot object moves across row . . . . .	34
4.6	Flowchart of processing . . . . .	35
4.7	Unified Knowledge Flow for all experiments . . . . .	40
4.8	Classifier Experiment Set 1 Setup . . . . .	43
4.9	Experiment Set 1 Class Distribution Before and After Weka Resampling . . . . .	44
A.1	Prototype in action . . . . .	56
A.2	Prototype Physical Form . . . . .	57

# List of Listings

3.1 Core feature extraction code . . . . .	27
--	----

## CHAPTER 1

# Introduction

The proportion of elderly and mobility-impaired people in the overall population is predicted to grow dramatically over the next century, leaving a large proportion of the population unable to care for themselves, and also reducing the proportion of the able-bodied population available to care for those individuals [8]. With this issue looming, serious investments need to be made into technologies that can provide the support these groups need to live independent of human assistance.

Additionally, the emergence of carbon pricing in many countries to combat anthropogenic climate change, as well as underinvestment in Australian energy infrastructure, are causing rising energy prices. These prices have a particularly large effect on the elderly and disabled, as they generally have quite low incomes.

Coinciding with these issues is the booming embedded systems and sensor industries, which are creating increasingly smaller computer and sensing systems. Each iteration, these systems become more powerful, more affordable, and more networked. This phenomena, termed the Internet of Things (IoT), has produced sub-\$50 devices such as the Arduino and Raspberry Pi which unlock enormous potential to create embedded systems to help combat these and other issues. One can envision a future ‘smart home for the disabled’ which leverages the IoT to offer a variety of services to help reduce financial and physical burdens alike.

Sensing techniques to determine occupancy, the detection of the presence and number of people in an area, are of particular use to the elderly and disabled. Detection can be used to inform various devices that change state depending on the user’s location, providing a variety of useful automations. In particular, such a system could better regulate energy hungry devices to help reduce financial burden. Household climate control, which in some regions of Australia accounts for up to 40% of energy usage [5] is one area in which occupancy detection can reduce costs. Several papers have found efficiency can be significantly increased, with some approaches providing annual energy savings of up to 25% [7].

There exist a great many cheap sensors in this field that offer the capacity to predict occupancy. However, in many cases they suffer from problems of installa-

tion logistics, difficult assembly, assumptions on user's technology ownership and component cost. In a smart home for the disabled, accuracy is important, but accessibility is paramount.

In this research project, we construct an IoT-style occupancy detection sensor system that forms part of a theoretical 'smart home for the disabled.' This system must meet the following qualitative accessibility criteria;

- *Low Cost:* The set of components required should aim to minimise cost, as these devices are intended to be deployed in situations where the serviced user may be financially restricted.
- *Non-Invasive:* The sensors used in the system should gather as little information as necessary to achieve the detection goal; there are privacy concerns with the use of high-definition sensors.
- *Reliable:* The system should be able to operate without user intervention or frequent maintenance, and should be able to perform its occupancy detection goal with a high degree of accuracy.
- *Energy Efficient:* The system may be placed in a location where there is no access to mains power, or where the retrofitting of appropriate power interfaces can be expensive (such as a residential roof); the ability to survive for long periods on only battery power is advantageous.

Constructing a sensor system that meets these criteria involves a four step process outlined below. Each of these steps is dedicated a chapter in this dissertation.

1. *Literature Review:* An extensive literature review will be performed of the field of occupancy detection to determine which sensors types are most apparently appropriate for occupancy detection given the above criteria.
2. *Design:* Once the most appropriate sensor type is determined, a hardware and software prototype will be developed to provide a platform for experimentation and evaluation of the sensor, as well as to capture, store, visualize and replay sensor data for those purposes.
3. *Evaluation:* Once a prototype exists, a methodology will be developed to evaluate the properties of the sensor, and experiments will be designed and conducted to test different algorithms effectiveness in using the prototype for occupancy detection.
4. *Conclusion:* The prototype's experimental results will be analyzed to conclude as to its effectiveness with relation to the above criteria.

## CHAPTER 2

# Literature Review

Within this chapter we consider the broad variety of sensing systems available, and how well existing solutions meet our sensing criteria. It can be difficult to approach the board variety of sensor types in the field, so a structure must be developed through which to evaluate them. Teixeira, Dublon and Savvides [20] propose a 5-element human-sensing criteria which provides a structure through which we may define the broad quantitative requirements of different sensors.

These quantitative requirements can be used to exclude sensing options that clearly cannot meet the requirements before the more specific qualitative accessibility criteria will be considered for those remaining sensors.

The quantitative criteria elements are;

1. *Presence*: Is there any occupant present in the sensed area?
2. *Count*: How many occupants are there in the sensed area?
3. *Location*: Where are the occupants in the sensed area?
4. *Track*: Where do the occupants move in the sensed area? (local identification)
5. *Identity*: Who are the occupants in the sensed area? (global identification)

At a fundamental level, this research project requires a sensor system that provides both Presence and Count information. To assist with the reduction of privacy concerns, excluding systems that permit Identity will generally result in a less invasive system also. The presence of Location or Track are irrelevant to our project's goals, but overall, minimizing these elements should in most cases help to maximize the energy efficiency of the system also.

Teixeira, Dublon and Savvides [20] also propose a measurable occupancy sensor taxonomy (see Figure 2.1 on the following page), which categorizes different

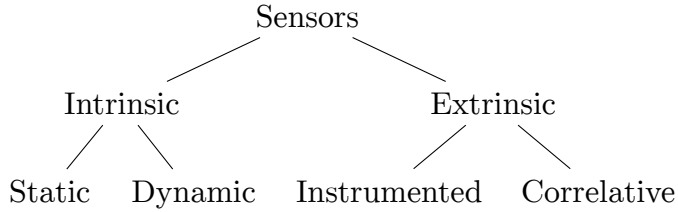


Figure 2.1: Taxonomy of occupancy sensors

sensing systems in terms of what information they use as a proxy for human-sensing. We use this taxonomy here as a structure through which we group and discuss different sensor types.

## 2.1 Intrinsic traits

Intrinsic traits are those which can be sensed that are a direct property of being a human occupant. Intrinsic traits are particularly useful, as in many situations they are guaranteed to be present if an occupant is present. However, they do have varying degrees of detectability and differentiation between occupants. Two main subcategories of these sensor types are static and dynamic traits.

### 2.1.1 Static traits

Static traits are physiologically derived, and are present with most (living) occupants. One key static trait that can be used for occupant sensing is that of thermal emissions. All human occupants emit distinctive thermal radiation in both resting and active states. The heat signatures of these emissions could potentially be measured with some apparatus, counted, and used to provide Presence and Count information to a sensor system, without providing Identity information.

Beltran, Erickson and Cerpa [7] propose Thermosense, a system that uses a type of thermal sensor known as an Infrared Array Sensor (IAS). This sensor is much like a camera, in that it has a field of view which is divided into “pixels”; in this case an  $8 \times 8$  grid of detected temperatures. This sensor is mounted on an embedded device on the ceiling, along with a Passive Infrared Sensor (PIR), and uses a variety of classification algorithms to detect human heat signatures within the raw thermal and motion data it collects. Thermosense achieves Root Mean Squared Error  $\approx 0.35$  persons, meaning the standard deviation between Thermosense’s occupancy predictions and the actual occupancy number was  $\approx 0.35$ .

Another static trait is that of CO<sub>2</sub> emissions, which, like thermal emissions, are emitted by human occupants in both resting and active states. By measuring the buildup of CO<sub>2</sub> within a given area, one can use a variety of mathematical models of human CO<sub>2</sub> production to determine the likely number of occupants present. Hailemariam et al. [12] trialled this as part of a sensor fusion within the context of an office environment, achieving a  $\approx 94\%$  accuracy. Such a sensing system could provide both the Presence and Count information, and exclude the Identity information as required. However, a CO<sub>2</sub> based detection mechanism has serious drawbacks, discussed by Fisk, Faulkner and Sullivan [10]: The CO<sub>2</sub> feedback mechanism is very slow, taking hours of continuous occupancy to correctly identify the presence of people. In a residential environment, occupants are more likely to be moving between rooms than an office, so the system may have a more difficult time detecting in that situation. Similarly, such systems can be interfered with by other elements that control the CO<sub>2</sub> buildup in a space, like air conditioners, open windows, etc. This is also much more of a concern in a residential environment compared to the studied office space, as the average residence can have numerous such confounding factors that cannot easily be controlled for.

Visual identification can be achieved through the use of video or still-image cameras and advanced image processing algorithms. Video can be used in occupancy detection in several different ways, achieving different levels of accuracy and requiring different configurations. The first use of video, POEM, proposed by Erickson, Achleitner and Cerpa [9] is the use of video as a “optical turnstile”; the video system detects potential occupants and the direction they are moving in at each entrance and exit to an area, and uses that information to extrapolate the number of occupants within the turnstiled area; this system has up to a 94% accuracy. However, the main issue with such a system applied to a residential environment is the system assumes that there will be wide enough “turnstile areas”, corridors of a fairly large area that connect different sections of a building, to use as detection zones. While such corridors exist in office environments, they are less likely to exist in residential ones.

Another video sensor system is proposed by Serrano-Cuerda et al. [18], that uses ceiling-based cameras and advanced image processing algorithms to count the number of people in the captured area. They measure accuracy using an F-score, which takes into account both false-positive and false-negative results, and is reported as 0.967, which is highly accurate. Such a system could be successfully applied to the residential environment, as both it and the “optical turnstile” model provide Presence and Count information. However, these systems also allow Identity to be determined, and thus are perceived as privacy-invasive. This perception leads to adoption and acceptance issues, which work against the ideal

system’s goals.

### 2.1.2 Dynamic traits

Dynamic traits are usually products of human occupant activity, and thus can generally only be detected when a human occupant is physically active or in motion.

Ultrasonic systems, such as Doorjamb proposed by Hnat et al. [13], use clusters of such sensors above doorframes to detect the height and direction of potential occupants travelling between rooms. This acts as a turnstile based system, much like POEM [9], but augments this with an understanding of the model of the building to error correct for invalid and impossible movements brought about from sensing errors. This system provides an overall room-level tracking accuracy of 90%, however to achieve this accuracy, potential occupants are intended to be tracked using their heights, which has privacy implications. The system can also suffer from problems with error propagation, as there are possibilities of “phantom” occupants entering a room due to sensing errors.

Solely PIR based systems, like those used by Hailemariam et al. [12], involve the motion of the sensor being averaged over several different time intervals, and fed into a decision tree classifier. This PIR system alone produced a  $\approx 98\%$  accuracy. However, such a system, due to only motion detection capabilities, can only provide Presence information, and is unable to provide Count information, nor detect motionless occupants.

## 2.2 Extrinsic traits

Extrinsic traits are those which are actually other environmental changes that are caused by or correlated with human occupant presence. These traits generally present a less accurate picture, or require the sensed occupants to be in some way “tagged”, but they are generally also easier to sense in of themselves. The sensors in this category have been divided into two subcategories.

### 2.2.1 Instrumented traits

One extrinsic trait category is instrumented approaches; these require that detectable occupants carry with them some device that is detected as a proxy for the occupant themselves.

The most obvious of these approaches is a specially designed device. Li et al. [16] use RFID tags placed on building occupant’s persons and a set of transmitters to triangulate the tags and place them within different thermal zones for the use of the HVAC system. For stationary occupants, there was a detection accuracy of  $\approx 88\%$ , and for occupants who were mobile, the accuracy was  $\approx 62\%$ . Such a system could be re-purposed for the residence, however, these systems raise issues in a residential environment as it requires occupants to be constantly carrying their sensors, which is less likely in such an environment. Additionally, the accuracy for this system is not necessarily high enough for a residential environment, where much smaller rooms are used.

To make extrinsic detection more reliable, Li, Calis and Becerik-Gerber [14] leverage a common consumer device; wifi enabled smart phones. They propose the *homeset* algorithm, which uses the phones to scan the visible wifi networks, and from that information estimate if the occupants are at home or out and about by “triangulating” their position from the visible wifi networks. This solution does not provide the fine-grained Presence data that we need, as it is only able to triangulate the phone’s position very roughly with the wireless network detection information.

Balaji et al. [6] also leverage smart phones to determine occupancy, but in a more broad enterprise environment: Wireless association logs are analysed to determine which access points in a building a given occupant is connected to. If this access point falls within the radio range of their designated “personal space”, they are considered to be occupying that personal space. This technique cannot be applied to a residential environment, as there are usually not multiple wireless hotspots.

Finally, Gupta, Intille and Larson [11] use specifically the GPS functions of the smartphone to perform optimisation on heating and cooling systems by calculating the “travel-to-home” time of occupants at all times and ensuring at every distance the house is minimally heated such that if the potential occupant were to travel home, the house would be at the correct temperature when they arrived. While this system does achieve similar potential air-conditioning energy savings, it is not room-level modular, and also presupposes an occupant whose primary energy costs are from incorrect heating when away from home, which isn’t necessarily the case for this demographic.

### 2.2.2 Correlative traits

The second of these subcategies are correlative approaches. These approaches analyse data that is correlated with human occupant activity, but does not require

	Requires		Excludes	Irrelevant	
	Presence	Count		Location	Track
<u>Intrinsic</u>					
<u>Static</u>					
Thermal	✓	✓	✓	✓	
CO <sub>2</sub>	✓	✓	✓		
Video	✓	✓	✗	✓	✓
<u>Dynamic</u>					
Ultrasonic	✓	✓	✗		✓
PIR	✓	✗	✓		
<u>Extrinsic</u>					
<u>Instrumented</u>					
RFID	✓ <sup>1</sup>	✓	✓	✓	
WiFi assoc. <sup>2</sup>	✓ <sup>1</sup>	✓	✗	✓	
WiFi triang. <sup>2</sup>	✓ <sup>1</sup>	✓	✗		
GPS <sup>2</sup>	✓ <sup>1</sup>	✗	✓	✓	
<u>Correlative</u>					
Electricity	✓ <sup>1</sup>	✗	✓		

<sup>1</sup>Doesn't provide data at required level of accuracy for home use.

<sup>2</sup>Uses smartphone as detector.

Table 2.1: Comparison of different sensors and project requirements

a specific device to be present on each occupant that is tracked with the system.

The primary approach in this area is work done by Kleiminger et al. [15], which attempts to measure electricity consumption and use such data to determine Presence. Electricity data was measured at two different levels of granularity; the whole house level with a smart meter, and the consumption of specific appliances through smart plugs. This data was then processed by a variety of classifiers to achieve a classification accuracy of more than 80%. Such a system presents a low-cost solution to occupancy, however it is not sufficiently granular in either the detection of multiple occupants, or the detection of occupants in a specific room.

## 2.3 Analysis

From these various sensor options, there are a few candidates that provide the necessary quantitative criteria (Presence and Count); these are thermal, CO<sub>2</sub>,

Video, Ultrasonic, RFID and WiFi association and triangulation based methods. All sensing options are compared on Table 2.1 on the previous page.

In the context of our four qualitative accessibility criteria, CO<sub>2</sub> sensing has several reliability drawbacks, the predominant ones being a large lag time to receive accurate occupancy information and interference from a variety of air conditioning sources which can modify the CO<sub>2</sub> concentration in the room in unexpected ways.

Video-based sensing methods suffer from invasiveness concerns, as they by design must have a constant video feed of all detected areas.

Ultrasonic methods suffer from reliability concerns when a user falls outside the prescribed height bounds of normal humans. Wheelchair bound occupants, a core demographic of our proposed sensing system, are not discussed in the Door-jamb paper. Their wheelchair may also interfere with height measurement results. Ultrasonic methods also provide weak Identity information through height detection.

RFID sensing also has several drawbacks; it is difficult value proposition to get residential occupants to carry RFID tags with them continuously. Another drawback is that the triangulation methods discussed are too unreliable to place occupants in specific rooms in many cases.

WiFi association is not granular enough for residential use, as the original enterprise use case presupposed a much larger area, as well as multiple wireless access points, neither of which a typical residential environment have.

WiFi triangulation is a good candidate for residential use, as there are most likely neighbouring wireless networks that can be used as virtual landmarks. However, it suffers from the same granularity problems as WiFi association, as these signals are not specific enough to pinpoint an occupant to a specific room.

For approaches presupposing smartphones being present on each occupant, it is more difficult to ensure that occupants are carrying their smartphones with them at all times in a residential environment. Another issue with smart phones is that they represent an expense that the target markets of the elderly and the disabled may not be able to afford.

Finally, we have thermal sensing. It provides both Presence and Count information, as it uses occupants' thermal signatures to determine the presence of people in a room. It does not however provide Identity information, as thermal signatures are not sufficiently unique with the technologies used to distinguish between occupants. Such a sensor system is presented as low-cost and energy efficient within Thermosense [7], is non-invasive by design and can reliably detect occupants with a very low root mean squared error. For our specific accessibility

criteria, thermal sensing appears to be the best option available.

## 2.4 Thermosense

Our analysis (Subsection 2.3 on page 8) concluded that thermal sensors are the best candidates for this project, with the state of the art in the field being Beltran, Erickson and Cerpa's Thermosense system. Using a similar Infrared Array Sensor (IAS) system along with those types of classification algorithms should yield useful sensing results which can be then integrated into the broader sensor system.

The Thermosense approach combines a Passive Infrared Sensor (PIR), which detects motion, and an IAS, which creates a thermal image to determine occupancy. The specific IAS used subdivides the visible area into an  $8 \times 8$  grid of sections from which temperatures can be derived. This sensor system is attached to the roof on a small embedded controller which is responsible for collecting the data and transmitting it back to a larger computer via a low powered wireless protocol.

Occupants are separated from background radiation through the use of a thermal background map. If no motion is detected, this map is updated using a slow-moving Exponential Weighted Moving Average (EMWA) over a 15 minute time window. If the room remains occupied for a long period, a more complex scaling algorithm is used which considers the coldest points in the room empty, and averages them against the new background, then performs EMWA with a lower weighting.

### 2.4.1 Classification Algorithms

Machine learning classification, the use of algorithms and training data to generate programs that can make predictions, is a large part of the Thermosense paper. Here we discuss the different classification techniques that Thermosense uses, as well as discussing other common classification techniques that would offer useful comparison benchmarks.

Classification techniques can be split into two different classes of techniques; numeric and nominal. Numeric techniques provide predictions that are numerical in nature, that is, they return results on a continuous number line. Nominal techniques provide predictions whereby a new data point predicted to belong to one of a set of predetermined classes, for example, colours of the rainbow.

Classification algorithms make predictions by taking in a set of examples that

have the correct answer attached. The set of values that describe each example are known as feature vectors.

The aforementioned background map is used as a baseline to calculate standard deviations of each grid area, which are then used to determine several characteristics to be used as feature vectors for a variety of classification approaches. The determination of the feature vectors was subject to experimentation, since the differences at each grid element too susceptible to individual room conditions to be used as feature vectors. Instead, a set of three different features was designed; the number of temperature anomalies in the space, the number of groups of temperature anomalies, and the size of the largest anomaly in the space. These feature vectors were compared against three classification approaches; K-Nearest Neighbors, Linear Regression and an Artificial Neural Network. All three classifiers achieved a Root Mean Squared Error (RMSE) within  $0.38 \pm 0.04$ . This final classification is subject to a final averaging process over a 4 minute window to remove the presence of independent errors from the raw classification data.

In the Thermosense system, there exists a PIR whose purpose is to determine if there is currently motion in the detected area. This motion detection is averaged over a time window and is used by the Thermosense system to provide Presence information to the system. Because of this, it is not necessarily a requirement that cases with zero people are provided to the classification algorithms above, as the PIR alone can determine this information. Thermosense performed experimentation to determine if the classification was more accurate when instances of empty rooms were provided to the classification algorithm vs. not. They found that generally not providing the empty case to the classification algorithm improved accuracy.

One of the most common classification toolkits available is the open-source Weka, released by The University of Waikato, which provides toolkit of classification algorithms. We will discuss how to replicate these theoretical algorithms in terms of Weka.

#### 2.4.1.1 Neural Networks

An artificial neural network (ANN) uses neurons as a model for machine learning. A number of input neurons, in this case connected to the feature vectors, is fed into a network of neurons (the “hidden layer”), each of which has an activation function which determines what set of inputs will make it fire. This network then connects to a number of output neurons which can be queried to determine the network’s predicted result. In the nominal result case, there one neuron for each possible class, and in the numeric result case, there is one neuron without an

activation function that outputs the raw numerical estimate. Neural networks can approximate functions of nearly any complexity with sufficient neurons in the correct topology, and are a quite common classification technique.

Thermosense uses a neural network with a hidden layer of five neurons, with a sigmoid activation function for the hidden layer and a linear activation function for the output layer. They test only the one, two and three person cases, relying on their PIR to detect the zero person case. They use 70% of their data for training the neural net, 15% for testing the net and the final 15% for validating their results. Thermosense conducts tests interpreting the number of people as a numeric attribute.

We use Weka’s “MultilayerPerceptron” neural network, which creates a hidden layer of  $(\text{attributes} + \text{classes})/2$  (three) by default, however we manually reconfigure this to be one hidden layer of five neurons, like Thermosense. It uses a sigmoid activation function for all neurons, except in the case that a numerical answer is to be predicted, in which case like Thermosense, it uses a linear activation function for the output layer. As is standard, for validation we use a 10-fold cross-validation for our nominal approach, and attempt to replicate Thermosense’s configuration as closely as possible for the numeric result.

#### 2.4.1.2 k-nearest Neighbors

A  $k$ -nearest Neighbors (KNN) approach uses the topology of the training data as a means to classify future data. For each data point that requires classification, a majority vote of its  $k$  nearest neighbors in the training data determines which class it belongs to. KNN is one of the simplest machine learning algorithms, and due to its classification method, is highly sensitive to classes that overlap.

Thermosense uses 5-nearest Neighbors with the Euclidean distance between points. For determining the class label, higher weightings are given to training points inversely to their distance from the point being classified. Thermosense appears to use a nominal classification for their KNN.

We use Weka’s “iBk” function to perform a KNN calculation, configuring `distanceWeighting` to be “Weight by 1-distance” and KNN to be 5, to make the classification as similar in function to the Thermosense approach as is possible. Thermosense does not specify what validation technique they used, so we elected to use a standard 10-fold cross-validation.

#### 2.4.1.3 Linear Regression

A Linear Regression approach attempts to construct a linear equation to describe the relationship between a dependent variable (in this case, the number of people in the space), and a number of other indicator variables (in this case, the three feature vectors). Generally, the equation takes the form  $y = m_1x_1 + \dots + m_nx_n + c$ , where each of the feature vectors is multiplied by a weight, and then a final number is added to provide the final prediction.

Thermosense uses a Linear Regression model of  $y = \beta_A A + \beta_S S + \beta$ , whereby  $A$  is the number of active pixels,  $S$  is the size of the largest connected component, and the  $\beta$  values represent the corresponding coefficients. They opt to exclude the third feature, the number of connected components, as their testing indicates that excluding it minimizes the Root Mean Squared Error (RMSE) further.

We use Weka’s “LinearRegression” function, exclude the `numconnected` attribute from the feature vector list, to attempt to match this approach.

#### 2.4.1.4 Naive Bayes

A Naive Bayes approaches uses a simple application of Bayes’ probability theorem to construct a probability of a given value belonging to a given class taking into account what is already known about the distribution of each of the classes in the data set, and the classification of those points that surround the point needing classification. One of the disadvantages of the Naive Bayes approach (the source of its naivety) is that it assumes independence between each of the variables used for classification.

In our data, the assumption of independence of variables is not correct, as each of the features are slightly different representations of the same data. However, due to Naive Bayes’ ubiquity and simplicity, it can be illuminating to see how well a very common but poorly suited classifier fares with our data set. Within Weka, we use the “NaiveBayes” function, which has little by way of configuration, thus is left in its default state.

#### 2.4.1.5 Support Vector Machines

Support Vector Machines (SVM) attempt to classify data by trying to find a plane that best separates two classes in a higher dimensional space. They do this by determining “support vectors,” which are those data points that lie on the “edge” of the separation between classes, and then finding the plane that maximizes the margin between the two classes. We elected to test an SVM-based

approach to determine if our data set is particularly suited to classification by SVMs.

For our purposes, we use Weka’s “SMO” function, which implements the Sequential Minimal Optimization algorithm, an efficient and recent method of training SVMs. For datasets with more than two classes (such as ours), the “one vs. one” method is used, whereby an SVM is created for each pair of classes, and then a method of majority voting is used to determine which class is the ultimately correct one.

#### 2.4.1.6 Decision Trees

A Decision Tree based approach uses the concept of a decision tree to create effectively a list of logical conditions which when met cause a data point to be classified as a specific class. Decision Tree classifiers generally use a partitioning approach whereby they split the data using a specific metric to maximize the tree’s effectiveness. The advantages of Decision Trees are that they are considered to be “white boxes,” specifically meaning that the result that they generate is human readable. This is useful, as in addition to the classifier providing its prediction of which class suits the data best, the tree can also be inspected to determine if the decisions it has extrapolated appear to be sensible, and even tweaked by humans if necessary.

One quite common algorithm for generating decision trees is C4.5, which is implemented by the “J48” function in Weka. C4.5 uses a measure of information gain, a concept rooted in information theory and entropy, to determine when to create splits in the tree. There are few configurable parameters for this approach, and for those we use the Weka defaults.

#### 2.4.1.7 KStar

The KStar ( $K^*$ ) algorithm presents a change to the normal  $k$ -nearest Neighbors algorithm, in which the distance used to compare similar points is not the Euclidean distance, but rather an entropic distance. This has several positive effects; it makes the algorithm more robust to missing values, and also it makes the classifier able to output a numeric result in addition to or instead of a classification into a nominal class.

We have decided to use  $K^*$  as one of our classification algorithms as it presents an interesting and different approach, and also allows the investigation of KNN-like techniques in the numeric area.  $K^*$  is present in Weka as “KStar,” and we will opt to use it in its default state.

#### 2.4.1.8 0-R

0-R is our final classification algorithm. 0-R is a simple classifier that on nominal prediction will classify all new data as belonging to the category that was most common in the training data, and on numeric prediction will classify all new data as being the mean of all test data. A 0-R classifier, clearly, is not a serious classification technique, however it is useful in establishing a baseline from which to compare all other classification results.

In Weka, the 0-R classifier is known as “ZeroR” and accepts no parameters.

## 2.5 Research Gap

TODO: Describe how pre-existing sensors do not meet all the criteria, and how there is a research gap. Some sort of conclusion to tie it all together?

## CHAPTER 3

# Design and Implementation

With the Literature Review concluding that a design based on Thermosense would be most appropriate, a software and hardware prototype (the “sensing system”) must now be constructed to provide a platform for experimentation and evaluation of the sensor, as well as to capture, store, visualize and replay sensor data for those purposes. We will first discuss the hardware foundations of the project, then the architecture of the software developed to run on those foundations.

### 3.1 Hardware

As reliability and future extensibility are core concerns of the project, a three-tiered system is employed with regards to the hardware involved in the system (Table 3.1 on the next page). At the bottom, the Sensing Tier, we have the raw sensor. Connected to the sensors via those respective protocols is the Pre-processing Tier, run an embedded system. The embedded device polls the data from these sensors, performs necessary calculations to turn raw information into suitable data, and communicates this via Serial over USB to the third tier. The third tier, the Analysis Tier, is run on a fully fledged computer. In our prototype, it captures and stores both video data, and the Temperature and Motion data it receives over Serial over USB.

While at a glance this system may seem overly complicated, it ensures that a sensible upgrade path to a more feature-rich sensing system is available. In the current prototype, the Analysis Tier merely stores captured data for offline analysis, in future prototypes this analysis can be done live and served to interested parties over a RESTful API. In the current prototype, the Analysis and Sensing Tiers are connected by Serial over USB, in future prototypes, this can be replaced by a wireless mesh network, with many Preprocessing/Sensing Tier nodes communicating with one Analysis Tier node.

<b>Analysis Tier</b>	Raspberry Pi B+
<b>Preprocessing Tier</b>	Arduino Uno R3
<b>Sensing Tier</b>	Melexis MLX90620 & PIR

Table 3.1: Hardware tiers

### 3.1.1 Sensing

As discussed in the Literature Review, using an Infrared Array Sensor (IAS) appear to be the most viable way to achieve the high-level goals of this project. Thermosense [7], the primary occupancy sensor in the IAS space, used the low-cost Panasonic Grid-EYE sensor for this task. This sensor, costing around \$30USD, appears to be a prime candidate for use in this project, as it satisfied low-cost criteria, as well as being proven by Thermosense to be effective in this space. However, while still available for sale in the United States, we were unable to order the sensor for shipping to Australia due to export restrictions outside of our control. While such restrictions would be circumventable with sufficient effort, using a sensor with such restrictions in place goes against an implicit criteria of the parts used in the project being relatively easy to acquire.

This forced us to search for alternative sensors in the space that fulfill similar criteria but were more broadly available. The sensor we settled on was the Melexis MLX90620 (*Melexis*) [17], an IAS with similar overall qualities that differed in several important ways; it provides a  $16 \times 4$  grid of thermal information, it has an overall narrower field of view and it sells for approximately \$80USD. Like the Grid-EYE , the *Melexis* sensor communicates over the 2-wire I<sup>2</sup>C bus, a low-level bi-directional communication bus widely used and supported in embedded systems.

In an idealized version of this occupancy system, much like Thermosense this system would include wireless networking and a very small form factor. However, due to time and resource constraints, the scope of this project has been limited to a minimum viable implementation. Appendix Chapter ?? on page ?? discusses in detail how the introduction of new open standards in the Wireless Personal Area Network space could be used in future systems to provide robust, decentralized networking of future occupancy sensors. This prototype architecture has been designed such that a clear path to the idea system architecture discussed therein is available.

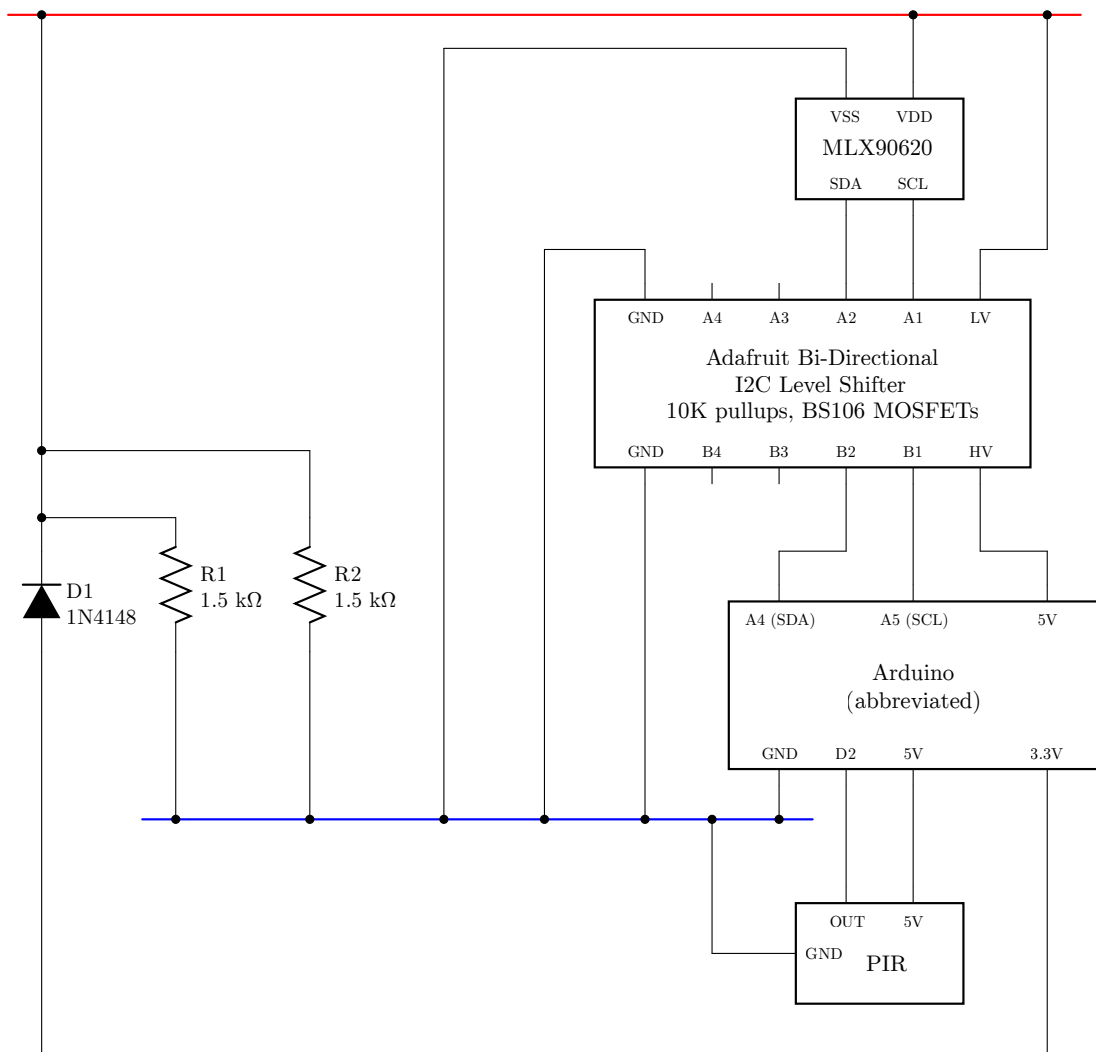


Figure 3.1: MLX90620, PIR and Arduino integration circuit

### 3.1.2 Pre-Processing

Due to low cost and ease of use, the Arduino platform was selected as the host for the Preprocessing Tier, and thus the low-level I<sup>2</sup>C interface for communication to the *Melexis*. Initially, this presented some challenges, as the *Melexis* recommends a power and communication voltage of 2.6V, while the Arduino is only able to output 3.3V and 5V as power, and 5V as communication. Due to this, it was not possible to directly connect the Arduino to the *Melexis*, and similarly due to the two-way nature of the I<sup>2</sup>C 2-wire communication protocol, it was also not possible to simply lower the Arduino voltage using simple electrical techniques, as such techniques would interfere with two-way communication.

A solution was found in the form of a I<sup>2</sup>C level-shifter, the Adafruit “4-channel I2C-safe Bi-directional Logic Level Converter” [1], which provided a cheap method to bi-directionally communicate between the two devices at their own preferred voltages. The layout of the circuit necessary to link the Arduino and the *Melexis* using this converter can be seen in Figure 3.1 on the previous page.

Additionally, as used in the Thermosense paper, a Passive Infrared Sensor (PIR) motion sensor [2] was also connected to the Arduino . This sensor, operating at 5V natively, did not require any complex circuitry to interface with the Arduino . It is connected to digital pin 2 on the Arduino , where it provides a rising signal in the event that motion is detected, which can be configured to cause an interrupt on the Arduino . In the configuration used in this project, the sensor’s sensitivity was set to the highest value and the timeout for re-triggering was set to the lowest value (approximately 2.5 seconds). Additionally, the continuous re-triggering feature (whereby the sensor produces continuous rising and falling signals for the duration of motion) was disabled using the provided jumpers.

### 3.1.3 Analysis / Classification

For the Analysis Tier, the Raspberry Pi B+ was chosen, as it is a powerful computer capable of running Linux available for an extraordinarily low price. The Arduino is connected to the Raspberry Pi over USB, which provides it both power and the capacity to transfer data. In turn, the Raspberry Pi is connected to a simple micro-USB rechargeable battery pack, which provides it with power, and subsequently the Arduino and sensors.

<b>Part</b>	<b>Cost (USD)</b>
MLX90620	\$80
Raspberry Pi B+	\$40
Raspberry Pi Camera	\$30
Arduino Uno R3	\$25
Passive Infrared Sensor	\$10
<b>TOTAL</b>	<b>\$185</b>

Table 3.2: Our project component costs

<b>Part</b>	<b>Cost (USD)</b>
Tmote Sky	\$100
Grid-EYE	\$30
Passive Infrared Sensor	\$10
<b>TOTAL</b>	<b>\$140</b>

Table 3.3: Thermosense component costs

### 3.1.4 Component Costs

As being low-cost is one of the project's goals, we have summarized the cost of each of the components of the prototype in Table 3.2. We believe that for a prototype, this cost is sufficiently low. In an ideal system, there would only be one Raspberry Pi in the system, and it would not require a camera, lowering the cost to around  $\$40 + n * \$115$  where  $n$  is the number of sensors. Similarly, as technology improves (as discussed in later chapters), sensor technology will continue to become cheaper, causing the most expensive component, the *Melexis*, to lower in cost.

When we compare this to the estimated cost of the Thermosense system (Table 3.3), we believe that it achieves a suitably comparable cost for a prototype. When removing the aspects of the prototype that would be unnecessary in the final version, the difference is less than \$15.

## 3.2 Software

At each layer of the described three-tier software architecture (pictured in greater detail in Figure 3.2 on page 22), there must exist software which governs the operation of that tier's processing concerns. Software in this project was written in two different languages.

At the Sensing Tier, it was not necessary for any software to be developed, as any software necessary came pre-installed and ready for use on the aforementioned sensors.

At the Preprocessing Tier, the Arduino, the default C++ derivative language was used, as careful management of memory usage and algorithmic complexity is required in such a resource-constrained environment, thus limiting choice in the area.

Finally, at Analysis Tier, a computer running fully-fledged Linux, choice of language becomes a possibility. In this instance, Python was settled on as the language of choice, as it is a quite high-level language with excellent library support for the functions required of the Analysis Tier, including serial interface, the use of the Raspberry Pi's built in camera, and image analysis. The 2.x branch of Python was chosen over the 3.x branch, despite its age, due a greater maturity in support for several key graphical interface libraries.

### 3.2.1 Sensing

TODO: MLX does sensing with internal software. Discuss architecture a little.

### 3.2.2 Pre-Processing

On the Arduino, once large program was developed, termed `mlx90620_driver.ino`. This program's purpose was to take simple commands over serial to configure the Melexis MLX90620 (*Melexis*) and to report back the current temperature values and Passive Infrared Sensor (PIR) motion information at either a pre-set interval, or when requested.

To calculate the final temperature values that the *Melexis* offers, a complex initialization and computational process must be followed, which is specified in the sensor's datasheet [17]. This process involves initializing the sensor with values attained from a separate on-board I<sup>2</sup>C EEPROM, then retrieving a variety of normalization and adjustment values, along with the raw sensor data, to compute the final temperature result.

The basic algorithm to perform this normalization was based upon the provided datasheet [17], as well as code by users "maxbot", "IIBaboomba", "nseidle" and others on the Arduino Forums [3] and was modified to operate with the newer Arduino "Wire" I<sup>2</sup>C libraries released since the authors' posts. In pursuit of the project's aims to create a more approachable thermal sensor, the code was also restructured and rewritten to be both more readable, and to introduce a set of

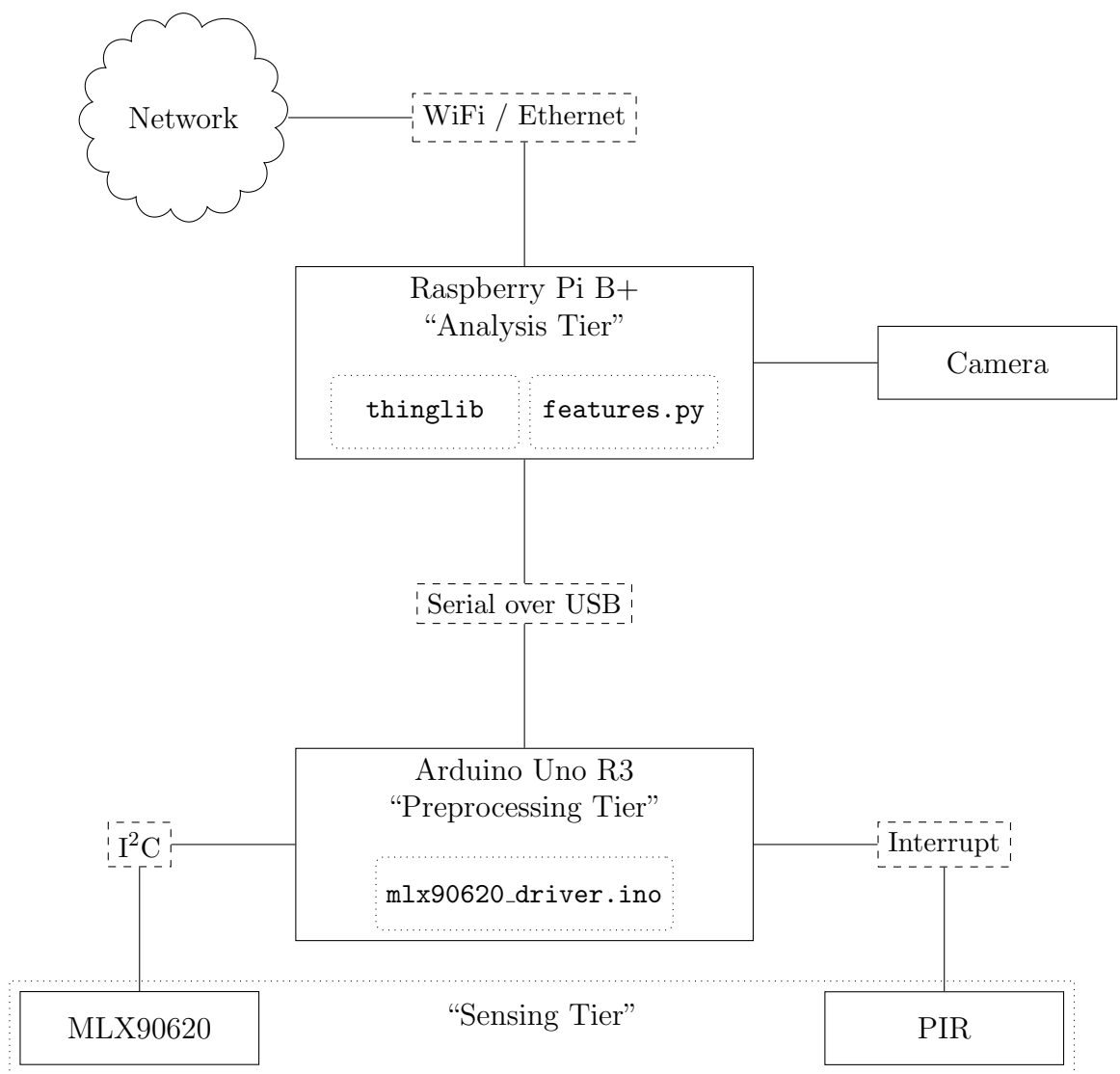


Figure 3.2: Prototype system architecture

```

INIT 0
INFO START
DRIVER MLX90620
BUILD Feb 1 2015 00:00:00
IRHZ 1
INFO STOP
ACTIVE 33

START 34
MOVEMENT 0
1.0 1.0 1.0 1.0 1.0 1.0 1.0 1.0 1.0 1.0 1.0 1.0 1.0 1.0 1.0 1.0
1.0 1.0 1.0 1.0 1.0 1.0 1.0 1.0 1.0 1.0 1.0 1.0 1.0 1.0 1.0 1.0
1.0 1.0 1.0 1.0 1.0 1.0 1.0 1.0 1.0 1.0 1.0 1.0 1.0 1.0 1.0 1.0
1.0 1.0 1.0 1.0 1.0 1.0 1.0 1.0 1.0 1.0 1.0 1.0 1.0 1.0 1.0 1.0
STOP 97

```

Figure 3.3: Initialisation sequence and thermal packet

features to make the management of the sensor data easier for the user, and for the information to be more human readable.

Additionally, support for the PIR’s motion data was added to the code, with the PIR configured to perform interrupts on one of the Arduino’s digital pin and the code structured to take note of this information and to report it to the user in the “MOTION” section of the next packet.

The first of the features introduced was the human-readable format for serial transmission. This allows the user to both easily write code that can parse the serial to acquire the serial data, as well as examine the serial data directly with ease. When the Arduino first boots running the software, Figure 3.3 is output. This specifies several things that are useful to the user; the attached sensor (“DRIVER”), the build of the software (“BUILD”) and the refresh rate of the sensor (“IRHZ”). Several different headers, such as “ACTIVE” and “INIT” specify the current millisecond time of the processor, thus indicating how long the execution of the initialization process took (33 milliseconds).

Once booted, the user is able to send several one-character commands to the sensor to configure operation, which are described in Table ?? on page ?? . Depending on the sensor configuration, IR data may be periodically output automatically, or otherwise manually triggered. This IR data is produced in the packet format described in Figure 3.3. This is a simple, human readable format that includes the millisecond time of the processor at the start and end of the calculation, if the PIR has seen any motion for the duration of the calculation, and the 16x4 grid of calculated temperature values.

### 3.2.3 Analysis / Classification

On the analysis tier a set of Python libraries and accompanying utility scripts were developed to interface with the Arduino, parse and interpret its data, and to provide data logging and visualization capabilities. Most of this functionality was split into a reusable and versatile Python module called **thinglib**.

**thinglib** provides 4 main feature sets across 3 files; the **Manager** series of classes, the **Visualizer** class, the **Features** class and the **pxdisplay** module.

#### Manager classes

The Manager series of classes are the direct interface between the Arduino and the Python classes. They implement a multi-threaded serial data collection and parsing system which converts the raw serial output of the connected Arduino into a series of Python data structures that represent the collected temperature and motion data of each captured frame. Several different versions of the **Manager** class exist to perform slightly different functions. When initializing these classes the sample rate of the *Melexis* can be configured, and it will be sent through to the Arduino for updating.

**BaseManager** is responsible for the implementation of the core serial parsing functions. It also provides a threaded interface through which the *Melexis*'s continuous stream of data can be subscribed to by other threads. The primary API, the **subscribe\_** series of functions, return a thread-safe queue structure, through which thermal packets can be received by various other threads when they become available.

**Manager**, the primary class, provides access the *Melexis*'s data at configurable intervals. When initializing this class, you may specify 0.5, 1, 2, 4 or 8Hz, and the class will configure the Arduino to both set the *Melexis* to this sample rate, and to automatically write this data to the serial buffer whenever it is available. This serial interface is multi-threaded, as at higher serial baud rates if data was not polled continuously enough the internal serial buffer would fill and some data would be discarded. By ensuring this process cannot be blocked by other parts of the running program this problem is mostly eliminated.

**OnDemandManager** operates in a similar way to **Manager**, however instead of using a non-blocking threaded approach, the user's scripts may request thermal/motion data from the class, and it will poll the Arduino for information and block until this information is parsed and returned.

Finally, **ManagerPlaybackEmulator** is a simple class which can take a previously created thermal recording from a file, and emulate the **Manager** class by

providing access to thread-safe queues which return this data at the specified Hz rate. This class can be used as a means to playback thermal recordings with the same visualization functions.

### `pxdisplay` functions

The `pxdisplay` module is a set of functions that utilize the `pygame` library to create a simple live-updating window containing a thermal map representation of the thermal data. One can generate any number of `pxdisplay` objects, which leverage the `multithreading` library and `multithreading.Queue` to allow thermal data to be sent to the display.

The class also provides a set of functions to set a “hotest” and “coldest” temperature and have RGB colors assigned from red to blue for each temperature that falls between those two extremes.

### `Visualizer` class

The `Visualizer` class is the natural compliment to the `Manager` series of classes. The functions contained within can usually be provided with a `Queue` object (generated by a `Manager` class) and can perform a variety of visualization and storage functions.

From the recording side, the `Visualizer` class can “record” a thermal capture by saving the motion and thermal information to a simple `.tcap` file, which stores the sample rate, timings, thermal and motion data from a capture in a very straightforward format. The class can also read these files back into the data structures `Visualizer` uses internally to store data. If `Visualizer` is running on a Raspberry Pi, it can also leverage the `picamera` library and the `OnDemandManager` class to synchronously capture both visual and thermal data for ground truth purposes.

From the visualization side, `Visualizer` can leverage the `pxdisplay` module to create thermal maps that can update in real-time based on the thermal data provided by a `Manager` class. The class can also generate both images and movie files from thermal recordings using the `PIL` and `ffmpeg` libraries respectively.

### `Features` class

In Thermosense [7], an algorithm was demonstrated that allowed the separation of “background” information from “active” pixels, and from that information,

the extraction of the features necessary for a classifier to correctly determine the number of people in an  $8 \times 8$  thermal image. This algorithm involved calculating the average and standard deviations of each pixel while it is guaranteed that the image would be empty, and then when motion is detected, considering any pixel “active” that reaches a value more than 3 standard deviations above the pixel when there was no motion.

From these “active” pixels, it was established that a set of three feature vectors were all that were required to correctly classify the number of people in the thermal image. These feature vectors were;

1. **Number of active pixels:** The total number of pixels that are considered “active” in a given frame
2. **Number of connected components:** If each active pixel is represented as an node in an undirected graph where adjacent active pixels are connected, how many connected components does this graph have?
3. **Size of largest connected component:** The number of active pixels contained within the largest connected component

In accordance with the pseudo-code outlined in the Thermosense paper, the algorithm described in Listing 3.1 on the following page was created to extract these figures. The portion of this code dealing with scaling the thermal background for rooms without motion was not implemented, as in all experiments tested, there exists a significant interval of time during which the no motion is guaranteed and the thermal background can be generated. The `networkx` library was used to generate the connected components information.

### 3.3 Conclusion

TODO: Some sort of summary here to tie things together? But what?

```

import networkx, itertools

nomotion_wgt = 0.01
n_rows = 4
n_cols = 16
background = first_frame
means = first_frame
stds = [ [0]*16 ]*4
stds_post = [ [None]*16 ]*4

def create_features(new_frame, is_motion):
    active = []
    g = networkx.Graph()

    for i, j in itertools.product( range(n_rows), range(n_cols) ):
        prev = background[i][j]
        cur = new_frame[i][j]
        cur_mean = means[i][j]
        cur_std = stds[i][j]

        if not is_motion:
            background[i][j] = nomotion_wgt * cur + (1 - nomotion_wgt) * prev
            means[i][j] = cur_mean + (cur - cur_mean) / n
            stds[i][j] = cur_std + (cur - cur_mean) * (cur - means[i][j])
            stds_post[i][j] = math.sqrt(stds[i][j] / (n-1))

        if (cur - background[i][j]) > (3 * stds_post[i][j]):
            active.append((i,j))
            g.add_node((i,j))

        # Add edges for nodes that have already been computed as active
        for ix, jx in [(-1, -1), (-1, 0), (-1, 1), (0, -1)]:
            if (i+ix, j+jx) in active:
                g.add_edge((i,j), (i+ix,j+jx))

    comps = list(networkx.connected_components(g))
    num_active = len(active)
    num_connected = len(comps)
    size_connected = max(len(c) for c in comps) if len(comps) > 0 else None

    return (num_active, num_connected, size_connected)

```

Listing 3.1: Core feature extraction code

## CHAPTER 4

# Evaluation

Now that the sensing system prototype has been realized, we are now able to perform experiments involving the system. In this chapter we create a set of experiments to test the sensor's properties and come to conclusions as to their effect on our ability to detect occupants. We then outline a process from taking raw sensor data and performing occupancy predictions with it. Using that process, we then devise a set of experiments involving recording occupancy data, and finally we process said data and produce accuracy results.

## 4.1 Sensor Properties

In order to best utilize the Melexis MLX90620 (*Melexis*), we must first understand the properties it exhibits, and their potential affects on our ability to perform person related measurements. These properties can be broadly separated into three different categories; bias, noise and sensitivity. A broad range of data was collected with the sensor in a horizontal orientation using various sources of heat and cold to determine these properties. This experimental setup is described in Figure 4.1 on the next page.

### 4.1.1 Bias

When receiving no infrared radiation, the sensor should indicate a near-zero temperature. If in such conditions it does not, that indicates that the sensor has some level of bias in its measurement values. We attempted to investigate this bias by performing thermal captures of the night sky. While this does not completely remove the infrared radiation, it does remove a significant proportion of it.

In Figure 4.2 on page 31 the thermal sensor was exposed to the night sky at a capture rate of 1Hz for 4 minutes, with the sensing results combined to create a

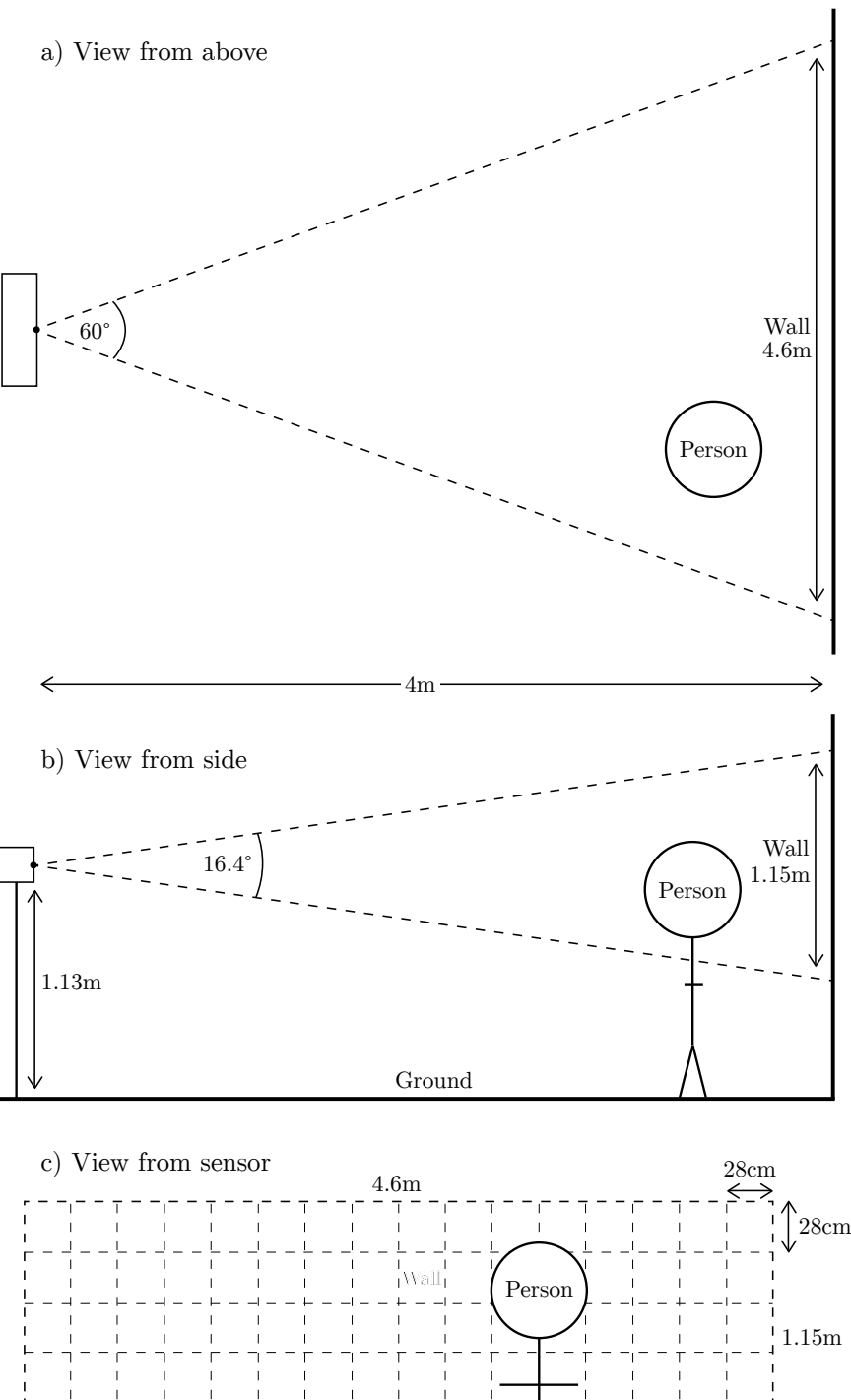


Figure 4.1: Experiment setup to determine sensor properties

set of means and standard deviations to indicate the pixels at “rest”. The average temperature detected was  $11.78^{\circ}\text{C}$ , with the standard deviation remaining less than  $0.51^{\circ}\text{C}$  over the entire exposure period. The resultant thermal map shows that pixels centered around the four “primary” pixels in the center maintain a similar temperature around  $9^{\circ}\text{C}$ , with temperatures beginning to deviate as they became further from the center.

The most likely cause of this bias is related to the physical structure of the sensor. The *Melexis* is a rectangular sensor which has been placed inside a circular tube. Due to this physical arrangement, the sides of this rectangular sensor will be significantly closer to these edges than the center. If these sides are at an ambient temperature higher than the measurement data (as they were in this case) thermal radiation from the sensor package itself could provide significant enough to cause the edges to appear warmer than the observed area of the sky. Such issues with temperature could be controlled for using a device that cools the sensor package to below that of the ambient temperature being measured, however, this is not a concern in this project, as the method of calculating a thermal background will compensate for any such bias as long as it remains constant.

#### 4.1.2 Noise

One of the features of the *Melexis* is the ability to sample the thermal data and a variety of sample rates between  $0.5\text{Hz}$  and  $512\text{Hz}$ . However, it was noted in early experimentation that a higher sample rate resulted in an increase in the noise contained within the resultant images. As our experiments focus on separating objects of interest from a thermal background, it is important to determine the maximum level of noise tolerable before our algorithms are unable to separate the background from the objects of interest.

Figure 4.3 on page 33 plots one of the central pixels of the sensor in a scenario where it is merely viewing a background (shown in green), and when it is viewing a person (shown in red), at the 5 different sample rates achievable with the current hardware. We can see in these plots that the data becomes significantly more noisy as the sample rate increases, and we can also determine that the sensor uses a form of data smoothing at lower sample rates, as the variance in data increases with sample rate.

If the sample rate were to increase, it is likely that the ability for the sensing system to disambiguate between objects of interest and the background would diminish. However, in the current project, even the slowest sampling rate of  $0.5\text{Hz}$  is sufficient, as occupancy estimations at a sub-second level present little

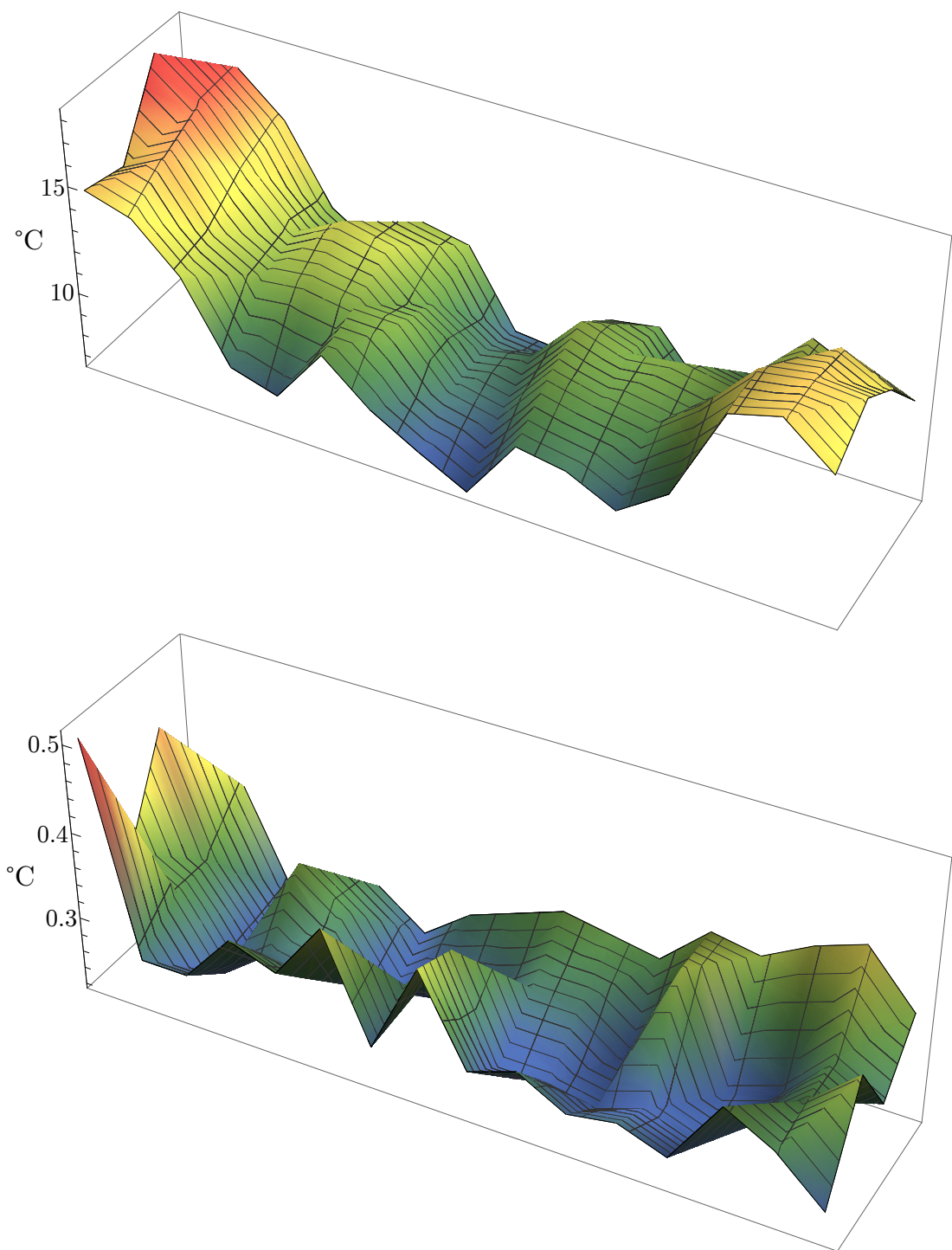


Figure 4.2: Plot of pixel means (top) and standard deviations (bottom) at rest

additional value and would require significant reforms in the efficiency of the software used.

### 4.1.3 Sensitivity

The *Melexis* is a sensor composed of 64 independent non-contact digital thermopiles, which measure infrared radiation to determine the temperature of objects. While they are bundled in one package, Figure 4.4 on page 34 shows that they are in fact wholly independent sensors placed in a grid structure. This has important effects on the properties of the data that the *Melexis* produces.

Figure 4.5 on page 34 shows a graph of the temperatures of the top row of 16 pixels of the *Melexis* as a hot object is moved from left to right at an approximately similar speed. One of the most interesting phenomena in this graph is the apparent extreme variability of the detected temperature of the object as it moves “between” two different pixels; there is a noticeable drop in the objects detected temperature. Further analysis of each of the pixel’s lines on the graph shows each pixel exhibiting a bell-curve like structure, with the detected temperature increasing from the baseline and peaking as the object enters the center of the pixel, and the detected temperature similarly decreasing as the object leaves the center.

This phenomenon has several possible causes. One likely explanation is that each individual pixel detects objects radiating at less favorable angles of incidence to be colder than they actually are: As the object enters a pixel’s effective field of view, it will radiate into the pixel at an angle that is at the edge of the pixel’s ability to sense, with this angle slowing decreasing until the hot object is directly radiating into the pixel’s sensor, causing a peak in the temperature reading. As the object leaves the individual elements field of view, the same happens in reverse.

While interesting, this phenomenon has little consequence to the effectiveness of the techniques used, as in experimental conditions the sensor will not be sufficiently distant that humans could be detected as single pixels. However, this phenomenon could be leveraged in future work to perform sub-pixel localization, discussed later on.

## 4.2 Energy Efficiency

TODO: This section will contain experimental descriptions relating to the power consumption of the prototype.

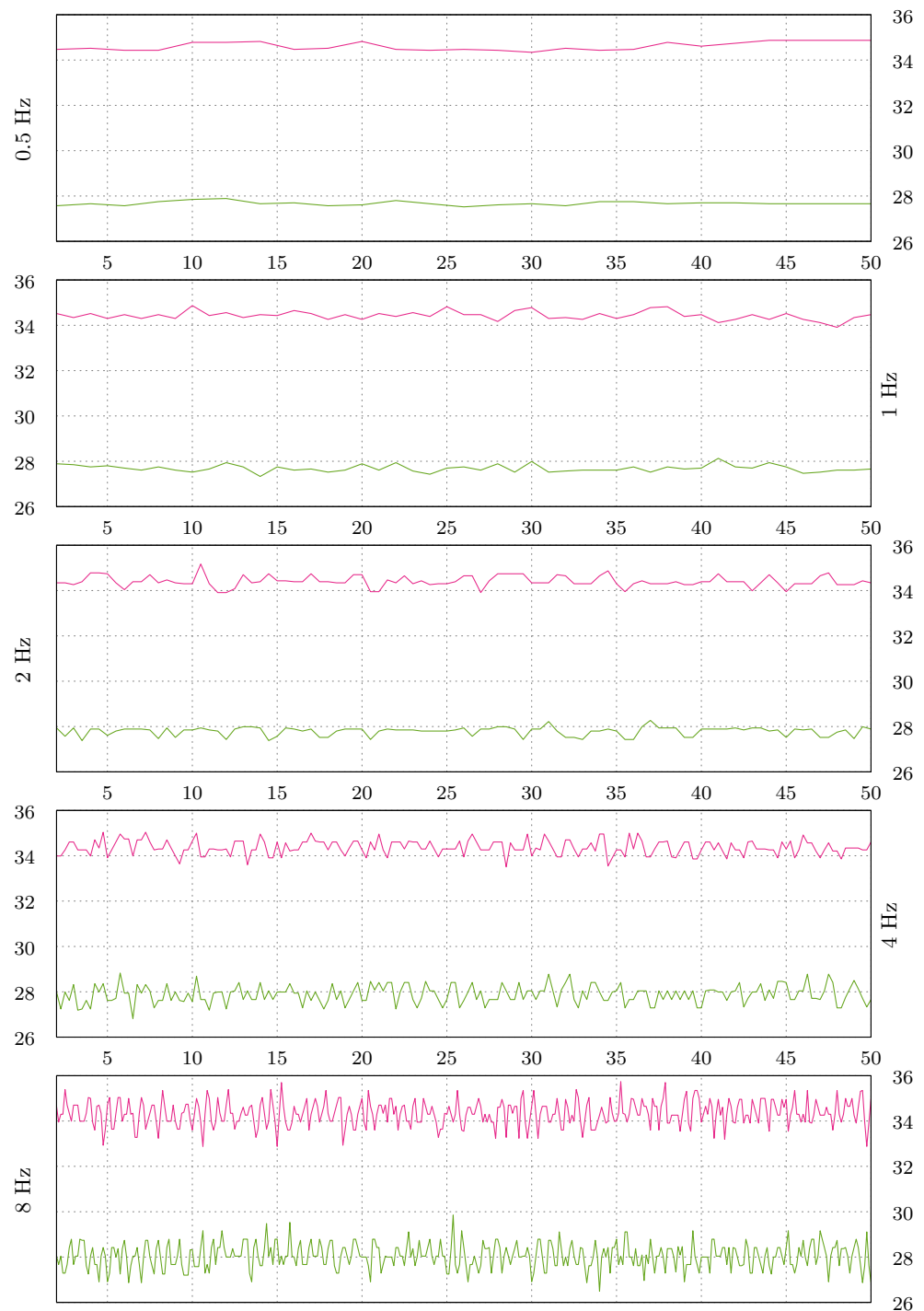


Figure 4.3: Noise levels of occupants (higher) and background (lower) at various sampling speeds

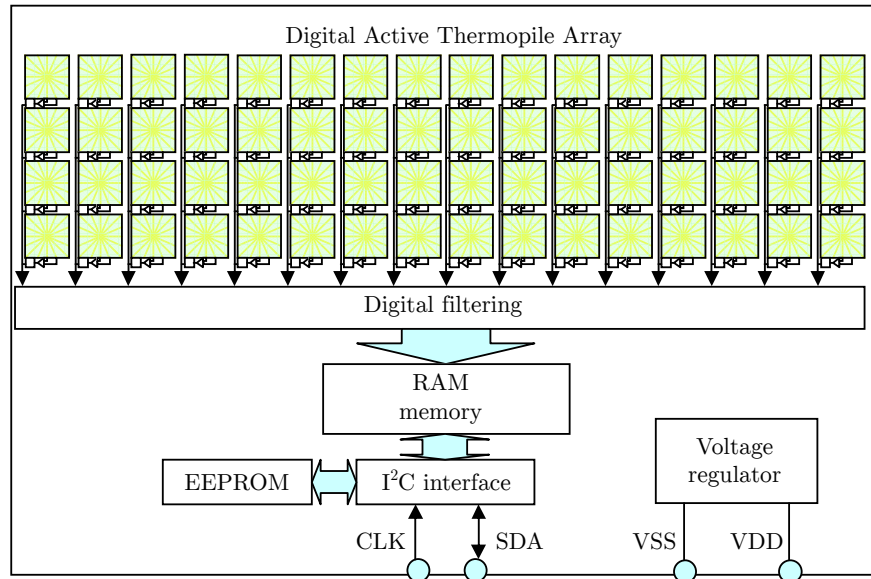


Figure 4.4: Block diagram for the *Melexis* taken from datasheet [17]

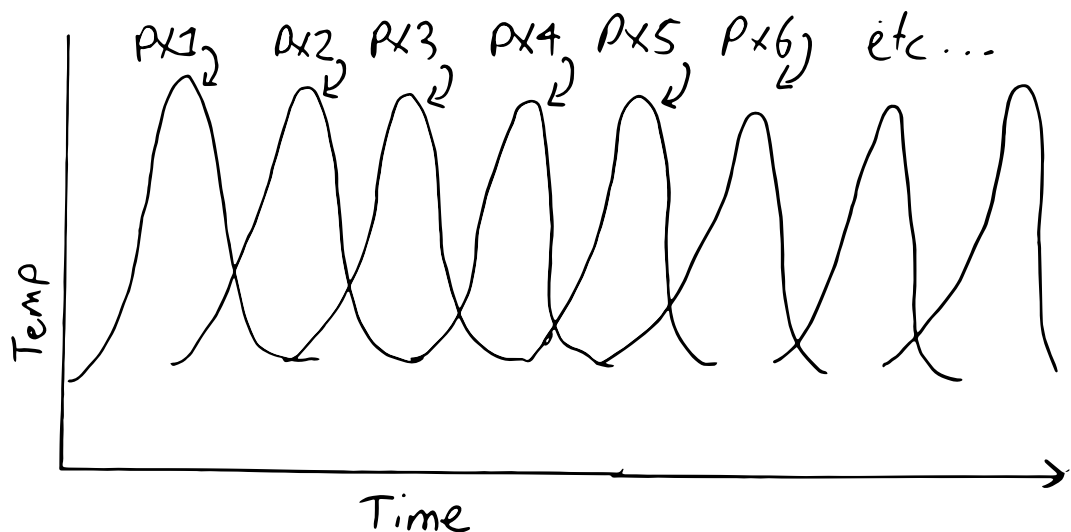


Figure 4.5: Different *Melexis* pixel temperature values as hot object moves across row

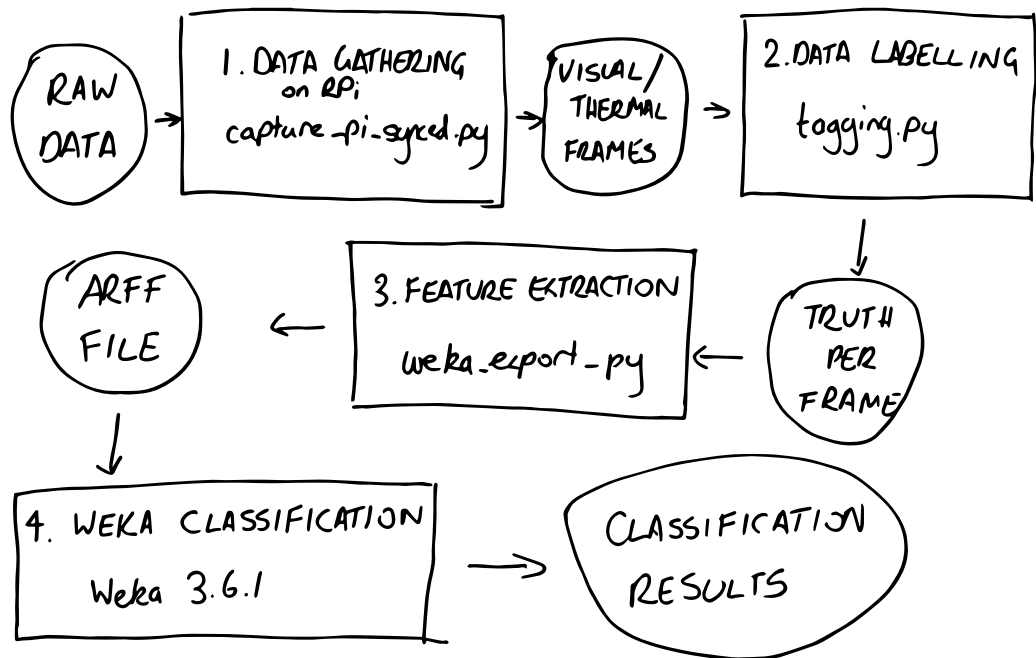


Figure 4.6: Flowchart of processing

### 4.3 Classification Accuracy

With the prototype, it is now possible to utilize the prototype to gather both thermal and visual data in a synchronized format. This data can be collected and used to determine the effectiveness of the human counting algorithms used. Due to the prototype's technical similarly to Thermosense [7], a similar set of experimental conditions will be used, with a comparison against Thermosense being used as a benchmark. To this end, several experiments were devised, each of which had its data gathered and processed in accordance with the same general process, outlined in Figure 4.6.

#### 4.3.1 Data gathering

As the camera and the Arduino are directly plugged into the Raspberry Pi, all data capture is performed on-board through SSH, with the data being then copied off the Pi for later processing. To perform this capture, the main script used is `capture_pi_synced.py`.

`capture_pi_synced.py` takes two parameters on the command line; the name of the capture output, and the number of seconds to capture. By default, it

always captures at 2Hz. The script initializes the `picamera` library, then passes a reference to it to the `capture_synced` function within the `Visualizer` class. The class will then handle the sending of commands to the Arduino to capture data in concert with taking still frames with the Raspberry Pi's camera.

When the script runs, it creates a folder with the name specified, storing inside a file named `output_thermal.hcap` containing the thermal capture, and a sequence of files with the format `video-%09d.jpg`, corresponding to each visual capture frame.

### 4.3.2 Data labeling

Once this data capture is complete, the data is copied to a more powerful computer for labeling. The utility `tagging.py` is used for this stage. This script is passed the path to the capture directory, and the number of frames at the beginning of the capture that are guaranteed to contain no motion. This utility will display frame by frame each visual and thermal capture together, as well as the computed feature vectors (based on a background map created from the first  $n$  frames without motion).

The user is then required to press one of the number keys on their keyboard to indicate the number of people present in this frame. This number will be recorded in a file called `truth` in the capture directory. The next frame will then be displayed, and the process continues. This utility enables the quick input of the ground truth of each capture, making the process more efficient.

### 4.3.3 Feature extraction and data conversion

Once the ground truth data is available, it is now possible to utilize the data to perform various classification tests. For this, we use version 3.7.12 of the open-source Weka toolkit [21], which provides easy access to a variety of machine learning algorithms and the tools necessary to analyze their effectiveness.

To enable the use of Weka, we export the ground truth and extracted features to a Comma Separated Value (CSV) file for processing. `weka_export.py` takes two parameters, a comma-separated list of different experiment directories to pull ground truth and feature data from, and the number of frames at the beginning of each capture that can be considered as "motionless." With this information, a CSV-file file is generated on which the heading indicating the attribute names is added for Weka to recognize.

#### 4.3.4 Running Weka Tests

Once the CSV file is generated, it is then possible to open the file in Weka for processing. Weka provides a variety of algorithms, but we choose a specific subset of algorithms based on those present in the Thermosense paper [7], as well others that we believe adequately represent the different approaches to classification.

Type	Attribute	Weka Class & Parameters
Neural Network (ANN)	Nominal, Numeric	weka.classifiers.functions.MultilayerPerceptron -L 0.3 -M 0.2 -N 500 -V 15 -S 0 -E 20 -H 5
<i>k</i> -nearest Neighbors (KNN)	Nominal, Numeric	weka.classifiers.lazy.IBk -K 5 -W 0 -F -A "weka.core.neighboursearch.LinearNNSearch -A \\"weka.core.EuclideanDistance -R first-last\\"
Naive Bayes	Nominal	weka.classifiers.bayes.NaiveBayes
Support Vector Machine (SVM)	Nominal	weka.classifiers.functions.SMO -C 1.0 -L 0.001 -P 1.0E-12 -N 0 -V -1 -W 1 -K "weka.classifiers.functions.supportVector.PolyKernel -C 250007 -E 1.0"
Decision Tree	Nominal	weka.classifiers.trees.J48 -C 0.25 -M 2
Entropy Distance	Nominal, Numeric	weka.classifiers.lazy.KStar -B 20 -M a
Linear Regression	Numeric	weka.classifiers.functions.LinearRegression -S 0 -R 1.0E-8
0-R	Nominal, Numeric	weka.classifiers.rules.ZeroR

Table 4.1: Weka parameters used for classifications

For those tests that are “nominal,” the `npeople` attribute was interpreted as nominal using the “NumericToNominal” filter, which creates a class for each value deleted in `npeople`’s columns. For those tests that are “numeric,” `npeople` is left unchanged, as by default all CSV import attributes are interpreted as such. For all tests where not specifically instructed, we use 10-fold cross-validation to validate our results.

As the data we are using is based on real experiments, the number of frames which are classified as each class may be unbalanced, which could cause the classification results to be affected. To that end, for each classification technique, we both classify the data in its raw, unbalanced form, and we also uniformly resample the `npeople` parameter using `weka.filters.supervised.instance.Resample -B 1.0 -S 1 -Z 100.0` in the pre-processing stage.

To help maximize the efficiency of the classification task, we use the Weka Knowledge Flow constructor to generate an encompassing flow that accepts an input CSV file of the raw data, and performs all resampling, numeric and nominal classification, returning a text file with the results of each of the different classification techniques run. The knowledge flow’s struture can be seen in . To enable maximum efficiency, the input and output elements of this flow are set to the environmental variables `UnifiedFlow.InputCSV` and `UnifiedFlow.OutputCSV`, a Jython script, `run_flow.py`, then sets those environmental variables to input and output file names, then calls the flow using Weka’s Java API. After this is complete, the script then runs a series of regexes on the output text data to generate summary spreadsheets with the relevant values.

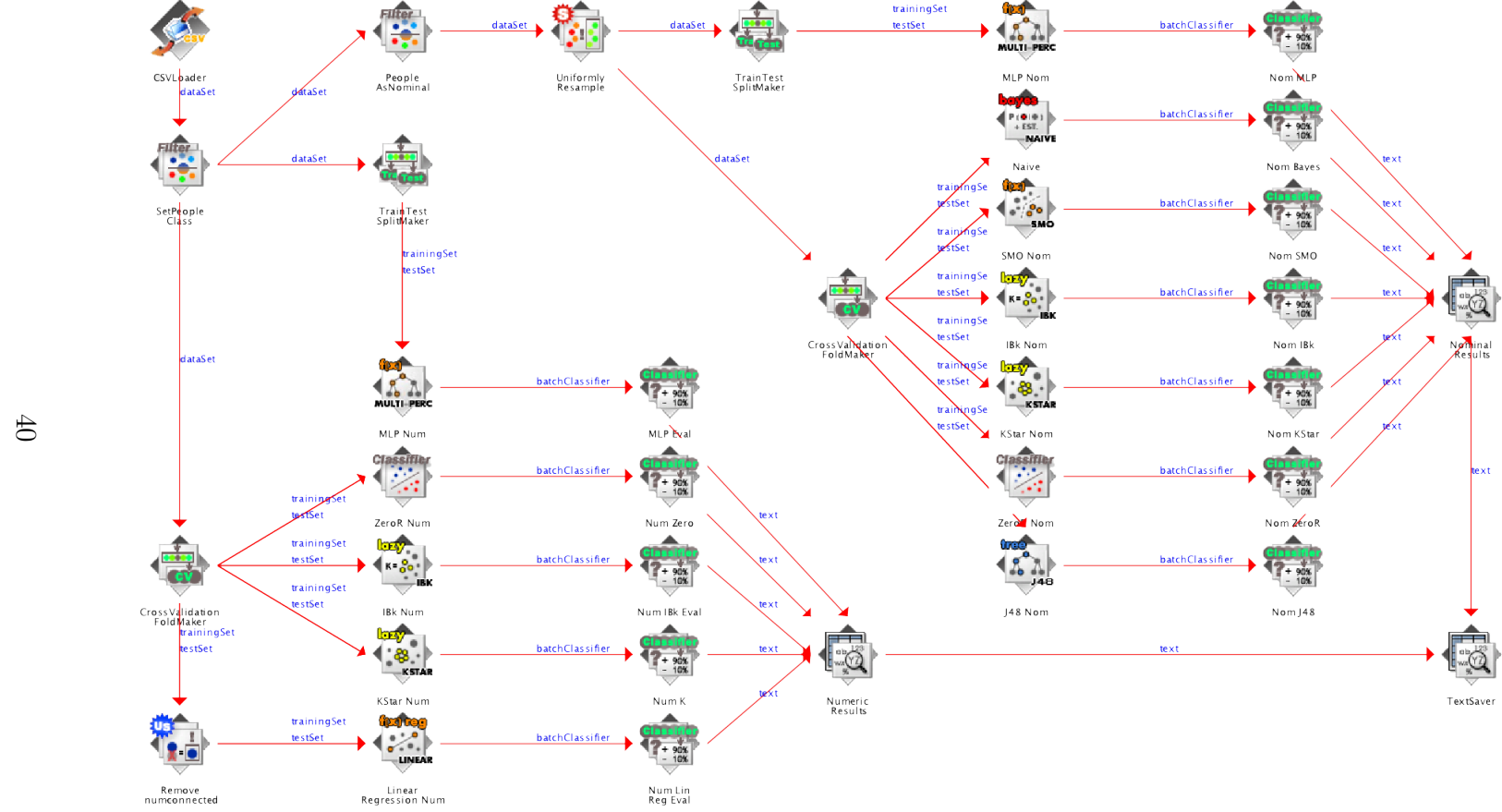


Figure 4.7: Unified Knowledge Flow for all experiments

### 4.3.5 Classifier Experiment Set 1

In our first set of experiments, a scene was devised in accordance with Figure 4.8 on page 43 that attempted to sense people from above, as did Thermosense. The prototype was set up on the ceiling, pointing down at a slight angle. For ease of use, the prototype was powered by mains power, and was networked with a laptop for command input and data collection via Ethernet. This set of experiments involved between zero and three people being present in the scene, moving in and out in various ways in accordance with the script in Table 4.2 on the following page.

1. (Remained standing) One person walks in, stands in center, walks out of frame. (sub-experiment 1)
2. (Remained standing) One person walks in, joined by another person, both stand there, one leaves, then another leaves. (sub-experiment 2)
3. (Remained standing) One person walks in, joined by one, joined by another, all stand there, one leaves, then another, then another. (sub-experiment 3)
4. (Remained standing) Two people walk in simultaneously, both stand there, both leave simultaneously. (sub-experiment 4)
5. (Sitting) One person walks in, sits in center, moves to right, walks out of frame. (sub-experiment 5)
6. (Sitting) One person walks in, joined by another person, both sit there, they stand and switch chairs, one leaves, then another leaves. (sub-experiment 6)
7. (Sitting) One person walks in, joined by one, joined by another, they all sit there, one leaves, one shuffles position, then another leaves, then another. (x2) (sub-experiment 7, 8)
8. (Sitting) Two people walk in, both sit there, both leave. (sub-experiment 9)

Table 4.2: Experiment Set 1 Script

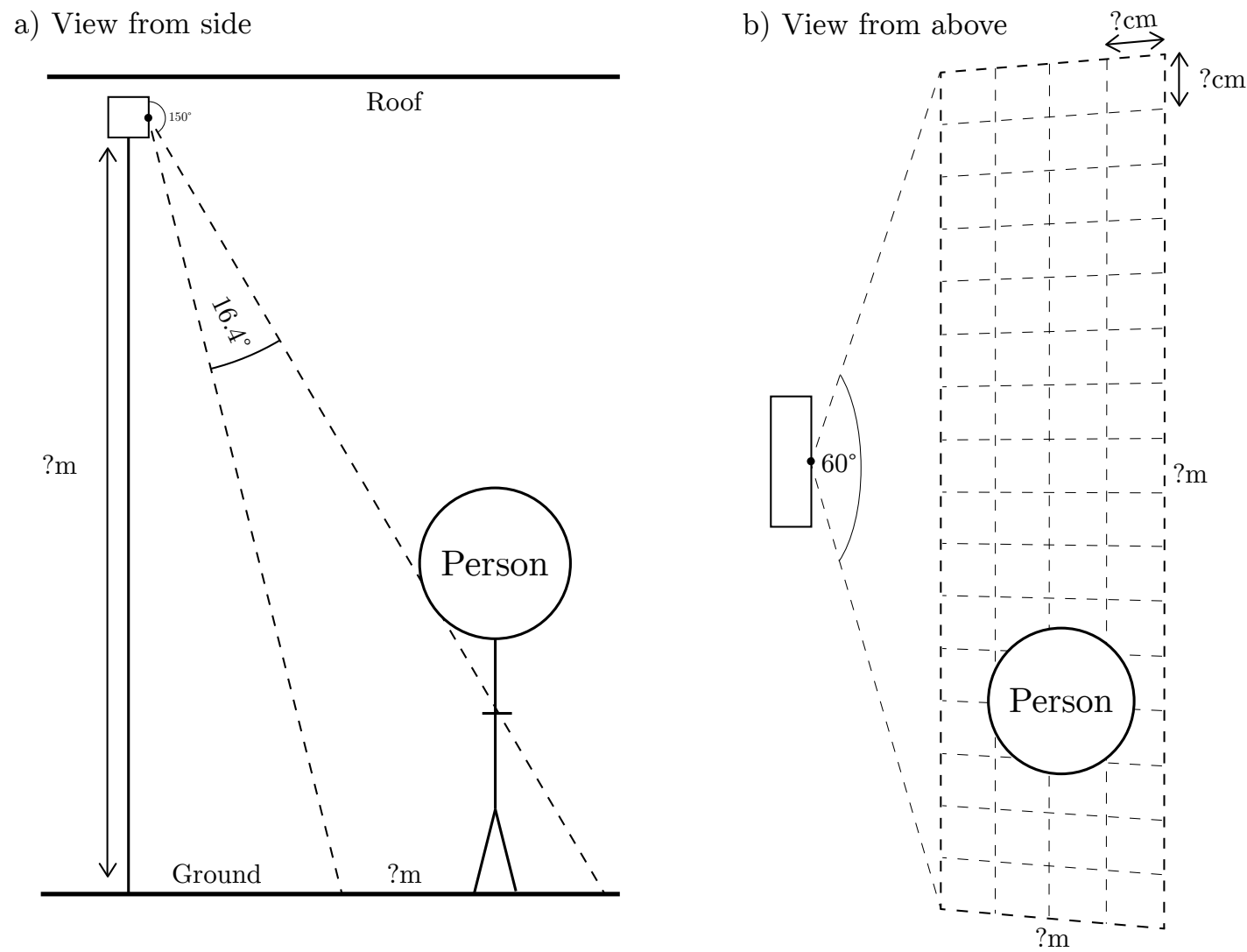


Figure 4.8: Classifier Experiment Set 1 Setup

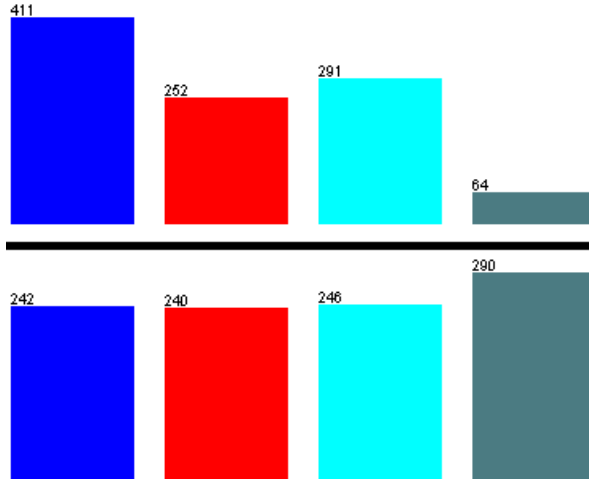


Figure 4.9: Experiment Set 1 Class Distribution Before and After Weka Resampling

In these experiments people moved slowly and deliberately, making sure there were large pauses between changes of action. The people involved were of average height, wearing various clothing. The room was cooled to 18 degrees for these experiments.

Each experiment was recorded with a thermal-visual synchronization at 1Hz over approximately 60-120 second intervals. Each experiment had 10-15 frames at the beginning where nothing was within the view of the sensor to allow the thermal background to be calculated. Each frame generated from these experiments was manually tagged with the ground truth value of its occupancy using the script mentioned previously.

The resulting features and ground truth were combined and exported to CSV allowing the Weka machine learning program to analyze them. This data was analyzed with the feature vectors always being considered numeric data and with the ground truth considered both numeric and nominal. All previously mentioned classification algorithms were run against the data set.

Experimental results from the first set of experiments were overall excellent, results from them can be seen in Table 4.3 on the next page. In the unbalanced results when including zero, an accuracy of 82.9% was observed, and in the balanced results, 78.2%. When excluding zero, the unbalanced results achieved 82.5% in the unbalanced and up to 84.9% in the balanced results.

Between the unbalanced and balanced classes when including zero, the ranking of different algorithms remained approximately the same, and consistently dropped in accuracy, with the exceptions being the SVM technique, which in-

Classifier	RMSE		% Excl. 0 Incl. 0		$R^2$ Excl. 0 Incl. 0	
	Excl. 0	Incl. 0	Excl. 0	Incl. 0	Excl. 0	Incl. 0
Thermosense Replication						
KNN (Nominal)	-	0.364	-	65.65	-	-
KNN (Numeric)	-	1.1235	-	-	-	0.3766
MLP	0.592	-	-	-	0.687	-
Lin Reg	0.525	-	-	-	0.589	-
Nominal Balanced						
C4.5	0.289	0.290	84.96	77.56	-	-
K*	0.296	0.293	84.27	78.25	-	-
MLP	0.359	0.320	70.86	72.13	-	-
Bayes	0.409	0.368	63.76	61.52	-	-
SVM	0.410	0.386	65.98	56.89	-	-
0-R	0.471	0.433	32.48	24.61	-	-
Numeric						
K*	0.423	0.550	-	-	0.760	0.828
0-R	0.651	0.972	-	-	-0.118	-0.129
Nominal Unbalanced						
C4.5	0.314	0.288	82.39	82.91	-	-
K*	0.304	0.285	82.56	82.61	-	-
MLP	0.362	0.286	77.14	78.69	-	-
Bayes	0.405	0.352	63.59	66.21	-	-
SVM	0.398	0.380	67.18	57.47	-	-
0-R	0.442	0.415	49.74	40.37	-	-

Table 4.3: Classifier Experiment Set 1 Results

creased in accuracy by about 1% in that instance. The drop in accuracy can be explained mostly by an over-representation of the zero class within the underbalanced data, as well as an underrepresentation of the three class (see Figure 4.9 on page 44). This is conformed by the fact that in the zero-excluded data, there is much less difference in the balanced and unbalanced set. These biases would enable classes to over-predict and under-predict these two classes respectively and achieve an artificially higher accuracy as a result. As discussed in the Methods, we performed re-sampling inside Weka to compensate for this.

For the numeric representation of the number of people, accuracy was consistently poor. From this data, we can see that all three classifiers used performed consistently poorly, with the Root Mean Square Errors being consistently double or more of comparable nominal results, and with correlation coefficients ( $R^2$ ) indicating poor (or in the case of KNN) very poor correlations.

The two highest accuracy classifiers, C4.5 and K\*, achieved quite similar results for both the balanced and unbalanced data while being quite different in implementation.

TODO: Discuss and compare this to ZeroR's RMSE. It's RMSE is quite close to some results, is this bad?

#### 4.3.5.1 Individual sub-experiment results

In addition to the above aggregate classification results, in which each of the nine sub-experiments results are combined and fed into the classifier, each of the sub-experiments has been individually classified with each of the six balanced nominal classifiers above. The results for these classifications can be seen in Table ?? on page ?? and Table 4.4 on the following page.

TODO: We talk about points of interest in the sub-experiment results and see if we can draw any useful conclusions from them.

	<b>1</b>	<b>2</b>	<b>3</b>	<b>4</b>	<b>5</b>	<b>6</b>	<b>7</b>	<b>8</b>	<b>9</b>	<b>Avg</b>
Nominal										
KNN	0.584	0.422	0.375	0.425	0.651	0.352	0.396	0.338	0.244	<i>0.421</i>
C4.5	0.342	0.270	0.278	0.414	0.456	0.267	0.318	0.288	0.250	<i>0.320</i>
K*	0.305	0.249	0.260	0.412	0.407	0.245	0.299	0.265	0.196	<i>0.293</i>
MLP	0.345	0.275	0.272	0.399	0.466	0.232	0.389	0.246	0.242	<i>0.318</i>
Bayes	0.391	0.359	0.290	0.435	0.473	0.276	0.381	0.306	0.243	<i>0.351</i>
SVM	0.447	0.447	0.379	0.444	0.602	0.378	0.380	0.377	0.335	<i>0.421</i>
Numeric										
0-R	0.500	0.471	0.433	0.472	0.500	0.471	0.433	0.433	0.472	<i>0.465</i>
KNN	0.726	0.707	1.044	0.934	0.593	0.531	0.899	0.585	0.829	<i>0.761</i>
K*	0.256	0.422	0.598	0.806	0.377	0.432	0.586	0.627	0.472	<i>0.508</i>
Lin Reg	0.270	0.635	0.623	0.821	0.422	0.508	0.589	0.708	0.570	<i>0.572</i>
MLP	0.379	0.460	0.500	0.868	0.399	0.306	0.790	0.490	0.406	<i>0.511</i>
0-R	0.409	0.762	1.009	0.986	0.507	0.829	1.014	1.043	1.012	<i>0.841</i>
Avg	<i>0.413</i>	<i>0.457</i>	<i>0.505</i>	<i>0.618</i>	<i>0.488</i>	<i>0.402</i>	<i>0.539</i>	<i>0.475</i>	<i>0.439</i>	

Table 4.4: Classifier Experiment Set 1 Individual Sub-experiment RMSEs

## 4.4 Thermosense Comparison and Discussion

To aid in comparison with the Thermosense algorithm, in our experiment sets we chose three techniques similar to those used in Thermosense; an Artificial Neural Network (Multilayer Perceptron in Weka),  $k$ -nearest Neighbors (IBk in Weka) and Linear Regression. Our results for our approximations to their algorithms can be seen in the Thermosense Replication section of Table 4.3 on page 45. We also use an experimental setup with 0–3 or 1–3 people, depending on the classifier, just as the Thermosense experiments do. For KNN, it was ambiguous if Thermosense used numeric or a nominal class attributes in their experiments, so we have performed both options above. The specifics of this is discussed in the Methods chapter.

For those experiments where we tried to specifically replicate Thermosense' results, we found consistently poor results that did not come close to meeting the  $R^2$  or RMSE values that Thermosense claimed. Their  $R^2$  values were in the 0.8 range, while ours range from around 0.3–0.7. This can be put down to a multitude of factors, with one likely explanation being that differences with the Melexis MLX90620 (*Melexis*)'s narrower field of view being difficult for Thermosense' specific algorithmic selections to deal with.

Our Linear Regression (Equation (4.1)) underperforms particularly when compared to Thermosense' (Equation (4.2)), as it fails to find an adequate way to weight the two variables, instead opting to basically exclude them from consideration by picking very small weights and adding a large constant factor. We get a correlation of  $R^2 = 0.589$  vs Thermosense'  $R^2 = 0.858$ .

$$n = 0.0456a + -0.024s + 1.1772 \quad (4.1)$$

$$n = 0.141a + -0.051s + 0.201 \quad (4.2)$$

However, for those algorithms we chose ourselves to test, we found results that were comparable or even better than Thermosense. Our nominally classed C4.5 decision tree achieved an balanced RMSE excluding zero of 0.289, compared to Thermosense' best result of 0.346. In the numeric classes, the K\* implementation achieved correlations in the same ballpark of 0.760 (excl. 0) and 0.828 (incl. 0), compared to Thermosense' best 0.906 for their ANN.

However, none of the techniques used by Thermosense proved to be the best out of those algorithms tried. The Neural Network and  $k$ -nearest Neighbors techniques represent the middle-of-the-road of our results, with both being bested by the C4.5 and K\* algorithms, which produced RMSEs of 0.289 and 0.298

respectively. Both these results are significantly better than Thermosense's best RMSE of 0.346 for  $k$ -nearest Neighbors, with our C4.5 algorithm representing a 28% improvement over that technique.

## CHAPTER 5

# Conclusions

The smart-home economy continues to grow, with automation being one of the main areas driving growth. The ability to detect people present within a space is an important smart-automation feature, with the implications for climate control energy efficiency alone being highly significant.

This project has attempted to create an occupancy detection system for such a smart home environment that meets four criteria; Low Cost, Non-Invasive, Energy Efficient and Reliable. Building such a system to commercial standards is outside of the scope of this project, however a prototype that attempts to prove the concepts involved was built and tested against these criteria. This prototype was based upon the ceiling-mounted thermal imaging approach of Thermosense [7], which after extensive analysis proved to be the best option given our criteria.

This prototype both validates the methods and results of the Thermosense paper, discovers key caveats surrounding the Thermosense approach, and also creates a software and hardware base on which future research into the area of occupancy in thermal imaging can be explored.

### 5.1 Accuracy

TODO: Summarize results.

As discussed in the Results section, the prototype developed achieves excellent reliability, citing accuracies in the 80% range.

### 5.2 Energy Efficiency

TODO: Summarize 4.3

### 5.3 Privacy

As discussed in the Literature Review, low-resolution thermal sensing provides the best trade-off between accuracy and invasiveness. Due to sensing in the infrared spectrum, it becomes significantly harder to surveil people in a malicious way, as many identifying features of people are not visible in the IR spectrum. This is compounded by the low resolution, which similarly assists in reducing the invasiveness of the sensor.

### 5.4 Cost

TODO: Summarize findings about cost

### 5.5 Future Directions

This project merely touched upon the area of thermal sensing and occupancy detection, and has laid the foundation for many more projects that build upon this original project. Some areas of future research are discussed here;

#### 5.5.1 Sub-pixel localization

Due to the overlapping bell-curve characteristics of the Melexis MLX90620 (*Melexis*)'s pixels, it may be possible to perform sub-pixel localization on objects within images.

#### 5.5.2 Improving Robustness

One of the main areas of the project that was not explored due to time was the introducing of a wireless mesh networking architecture to the project. Future prototypes would consist of an many-to-one relationship between the Sensing/Pre-processing tier and the Analysis tier. Exploring the best way to mesh network these components while maintaining all the pre-existing criteria of the project would be challenging. In Appendix Chapter ?? on page ?? we provide our thoughts on the potential structure this could take.

Similarly, the current prototype uses a breadboarded structure that increases the size of the prototype significantly, as well as reduces the reliability of the

prototype in the long-term. Converting the *Melexis* and PIR into a printed circuit board that fits onto the Arduino as a shield would both reduce the size of the prototype, as well as improving reliability for the future.

### 5.5.3 Field-of-view modifications

Several different techniques could be used to improve upon the field-of-view limitations of the *Melexis*, and exploring them and their cost/complexity implications would be useful. The first of these is applying a lens to the sensor, effectively expanding the field-of-view, but at the cost of distorting the image. Compensating for this distortion while maintaining accuracy presents an intriguing problem.

In another direction, using a motor with the *Melexis* to “sweep” the room, and thereby constructing a larger image of the space could also resolve the field-of-view issues. However, this approach also presents problems in stitching the images together in a sensible way, the distortion caused by rotating the sensor, as well as handing cases in which a fast-moving object is represented multiple times in the stitched image.

### 5.5.4 New Sensors

During this project, an updated version of our sensor, the MLX90621, was released. This version doubles the field-of-view in both the horizontal and vertical directions, addressing many of the problems encountered with the size of detection area in low-ceiling rooms. This version offers nearly complete backwards compatibility with the older version. Updating the project code-base to support it and re-running the experiments with the increased field-of-view to determine how much of an improvement it is would be interesting.

In addition to this, significantly higher resolution sensors are beginning to come to the market. The FLiR Lepton [19], which sells in a dev kit for \$350, offers an  $80 \times 60$  pixel sensor with a comparable field-of-view to the Grid-EYE. Exploring the increases in accuracy achievable though such significant increases in resolution would have significant contrion.

## 5.6 Final Stuff

TODO: Something to wrap up with?

# Bibliography

- [1] ADAFRUIT. 4-channel I2C-safe bi-directional logic level converter - BSS138 (product ID 757). <http://www.adafruit.com/product/757>. Accessed: 2015-01-07.
- [2] ADAFRUIT. PIR (motion) sensor (product ID 189). <http://www.adafruit.com/product/189>. Accessed: 2015-02-08.
- [3] ARDUINO FORUMS. Arduino and MLX90620 16X4 pixel IR thermal array. <http://forum.arduino.cc/index.php/topic,126244.0.html>, 2012. Accessed: 2015-01-07.
- [4] ATZORI, L., IERA, A., AND MORABITO, G. The internet of things: A survey. *Computer networks* 54, 15 (2010), 2787–2805.
- [5] AUSTRALIAN BUREAU OF STATISTICS. Household water and energy use, Victoria: Heating and cooling. Tech. Rep. 4602.2, October 2011. Retrieved October 6, 2014 from <http://www.abs.gov.au/ausstats/abs@.nsf/0/85424ADCCF6E5AE9CA257A670013AF89>.
- [6] BALAJI, B., XU, J., NWOKAFOR, A., GUPTA, R., AND AGARWAL, Y. Sentinel: occupancy based HVAC actuation using existing WiFi infrastructure within commercial buildings. In *Proceedings of the 11th ACM Conference on Embedded Networked Sensor Systems* (2013), ACM, p. 17.
- [7] BELTRAN, A., ERICKSON, V. L., AND CERPA, A. E. ThermoSense: Occupancy thermal based sensing for HVAC control. In *Proceedings of the 5th ACM Workshop on Embedded Systems For Energy-Efficient Buildings* (2013), ACM, pp. 1–8.
- [8] CHAN, M., CAMPO, E., ESTÈVE, D., AND FOURNIOLS, J.-Y. Smart homes - current features and future perspectives. *Maturitas* 64, 2 (2009), 90–97.
- [9] ERICKSON, V. L., ACHLEITNER, S., AND CERPA, A. E. POEM: Power-efficient occupancy-based energy management system. In *Proceedings of the 12th international conference on Information processing in sensor networks* (2013), ACM, pp. 203–216.

- [10] FISK, W. J., FAULKNER, D., AND SULLIVAN, D. P. Accuracy of CO<sub>2</sub> sensors in commercial buildings: a pilot study. Tech. Rep. LBNL-61862, Lawrence Berkeley National Laboratory, 2006. Retrieved October 6, 2014 from [http://eaei.lbl.gov/sites/all/files/LBNL-61862\\_0.pdf](http://eaei.lbl.gov/sites/all/files/LBNL-61862_0.pdf).
- [11] GUPTA, M., INTILLE, S. S., AND LARSON, K. Adding gps-control to traditional thermostats: An exploration of potential energy savings and design challenges. In *Pervasive Computing*. Springer, 2009, pp. 95–114.
- [12] HAILEMARIAM, E., GOLDSTEIN, R., ATTAR, R., AND KHAN, A. Real-time occupancy detection using decision trees with multiple sensor types. In *Proceedings of the 2011 Symposium on Simulation for Architecture and Urban Design* (2011), Society for Computer Simulation International, pp. 141–148.
- [13] HNAT, T. W., GRIFFITHS, E., DAWSON, R., AND WHITEHOUSE, K. Doorjamb: unobtrusive room-level tracking of people in homes using doorway sensors. In *Proceedings of the 10th ACM Conference on Embedded Network Sensor Systems* (2012), ACM, pp. 309–322.
- [14] KLEIMINGER, W., BECKEL, C., DEY, A., AND SANTINI, S. Inferring household occupancy patterns from unlabelled sensor data. Tech. Rep. 795, ETH Zurich, 2013. Retrieved October 6, 2014 from [http://eaei.lbl.gov/sites/all/files/LBNL-61862\\_0.pdf](http://eaei.lbl.gov/sites/all/files/LBNL-61862_0.pdf).
- [15] KLEIMINGER, W., BECKEL, C., STAAKE, T., AND SANTINI, S. Occupancy detection from electricity consumption data. In *Proceedings of the 5th ACM Workshop on Embedded Systems For Energy-Efficient Buildings* (2013), ACM, pp. 1–8.
- [16] LI, N., CALIS, G., AND BECERIK-GERBER, B. Measuring and monitoring occupancy with an RFID based system for demand-driven HVAC operations. *Automation in construction* 24 (2012), 89–99.
- [17] MELEXIS. Datasheet IR thermometer 16X4 sensor array MLX90620. <http://www.melexis.com/Asset/Datasheet-IR-thermometer-16X4-sensor-array-MLX90620-DownloadLink-6099.aspx>, 2012. Accessed: 2015-01-07.
- [18] SERRANO-CUERDA, J., CASTILLO, J. C., SOKOLOVA, M. V., AND FERNÁNDEZ-CABALLERO, A. Efficient people counting from indoor overhead video camera. In *Trends in Practical Applications of Agents and Multiagent Systems*. Springer, 2013, pp. 129–137.

- [19] SPARKFUN. FLiR Dev Kit. <https://www.sparkfun.com/products/13233>. Accessed: 2015-04-08.
- [20] TEIXEIRA, T., DUBLON, G., AND SAVVIDES, A. A survey of human-sensing: Methods for detecting presence, count, location, track, and identity. Tech. rep., Embedded Networks and Applications Lab (ENALAB), Yale University, 2010. Retrieved October 6, 2014 from [http://www.eng.yale.edu/enalab/publications/human\\_sensing\\_enalabWIP.pdf](http://www.eng.yale.edu/enalab/publications/human_sensing_enalabWIP.pdf).
- [21] UNIVERSITY OF WAIKATO. Weka. <http://www.cs.waikato.ac.nz/ml/weka/>. Accessed: 2015-03-10.



## APPENDIX A

# Physical Form

To enable the prototype to be easily mounted on the ceiling, the prototype was placed on a flat board with feet that would enable it to be screwed into a pole, and the pole extended to jam the sensor against the ceiling and the floor using the pole (Figure A.2 on the next page, Figure A.1). Due to a wireless module and battery pack being added to the Raspberry Pi, it was feasible for the sensor to operate entirely wirelessly for several hours. However, in most cases it was more convenient to operate using wired power and Ethernet.

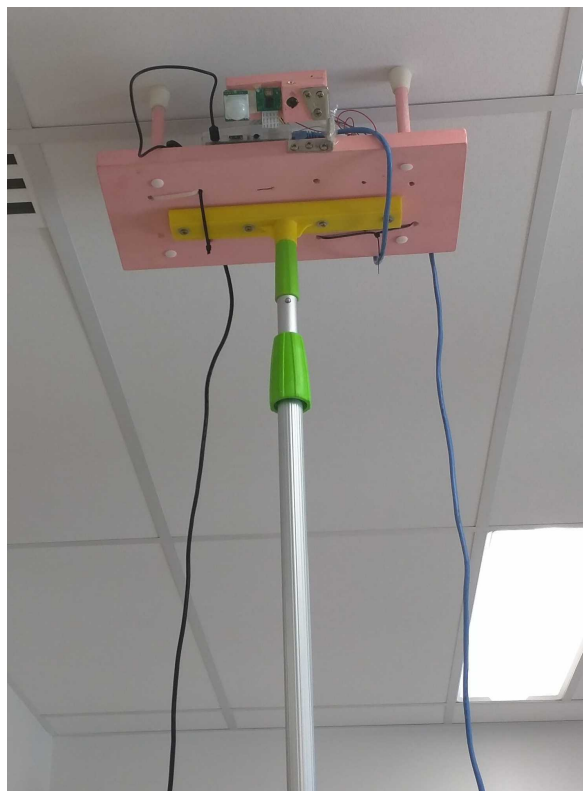
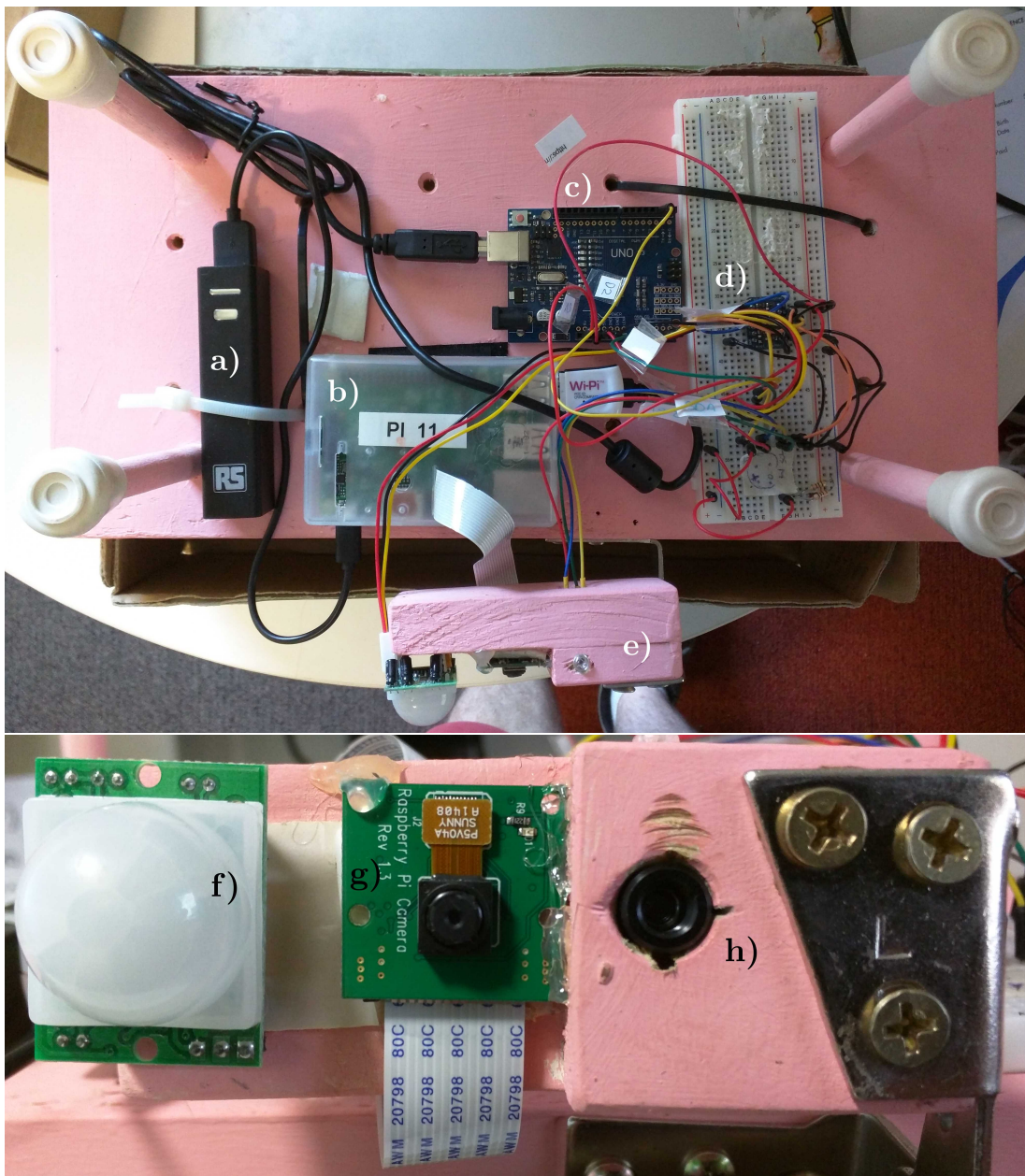


Figure A.1: Prototype in action



- |                             |  |
|-----------------------------|--|
| a) Battery pack             | e) Movable sensor mount                |
| b) Raspberry Pi             | f) PIR                                 |
| c) Arduino                  | g) Camera                              |
| d) Level-shifting circuitry | h) Melexis MLX90620 ( <i>Melexis</i> ) |

Figure A.2: Prototype Physical Form

## APPENDIX B

# Original Honours Proposal

**Title:** Developing a robust system for occupancy detection in the household

**Author:** Ash Tyndall

**Supervisor:** Professor Rachel Cardell-Oliver

**Degree:** BCompSci (24 point project)

**Date:** October 8, 2014

### B.1 Background

The proportion of elderly and mobility-impaired people is predicted to grow dramatically over the next century, leaving a large proportion of the population unable to care for themselves, and consequently less people able care for these groups. [5] With this issue looming, investments are being made into a variety of technologies that can provide the support these groups need to live independent of human assistance.

With recent advancements in low cost embedded computing, such as the Arduino [1] and Raspberry Pi, [14] the ability to provide a set of interconnected sensors, actuators and interfaces to enable a low-cost ‘smart home for the disabled’ is becoming increasingly achievable.

Sensing techniques to determine occupancy, the detection of the presence and number of people in an area, are of particular use to the elderly and disabled. Detection can be used to inform various devices that change state depending on the user’s location, including the better regulation energy hungry devices to help reduce financial burden. Household climate control, which in some regions of Australia accounts for up to 40% of energy usage [2] is one particular area

in which occupancy detection can reduce costs, as efficiency can be increased dramatically with annual energy savings of up to 25% found in some cases. [7]

Significant research has been performed into the occupancy field, with a focus on improving the energy efficiency of both office buildings and households. This is achieved through a variety of sensing means, including thermal arrays, [4] ultrasonic sensors, [10] smart phone tracking, [11][3] electricity consumption, [12] network traffic analysis, [15] sound, [9] CO<sub>2</sub>, [9] passive infrared, [9] video cameras, [6] and various fusions of the above. [16][15]

## B.2 Aim

While many of the above solutions achieve excellent accuracies, in many cases they suffer from problems of installation logistics, difficult assembly, assumptions on user's technology ownership and component cost. In a smart home for the disabled, accuracy is important, but accessibility is paramount.

The goal of this research project is to devise an occupancy detection system that forms part of a larger 'smart home for the disabled' that meets the following accessibility criteria;

- *Low Cost*: The set of components required should aim to minimise cost, as these devices are intended to be deployed in situations where the serviced user may be financially restricted.
- *Non-Invasive*: The sensors used in the system should gather as little information as necessary to achieve the detection goal; there are privacy concerns with the use of high-definition sensors.
- *Energy Efficient*: The system may be placed in a location where there is no access to mains power (i.e. roof), and the retrofitting of appropriate power can be difficult; the ability to survive for long periods on only battery power is advantageous.
- *Reliable*: The system should be able to operate without user intervention or frequent maintenance, and should be able to perform its occupancy detection goal with a high degree of accuracy.

Success in this project would involve both

1. Devising a bill of materials that can be purchased off-the-shelf, assembled without difficulty, on which a software platform can be installed that performs analysis of the sensor data and provides a simple answer to the occupancy question, and
2. Using those materials and softwares to create a final demonstration prototype whose success can be tested in controlled and real-world conditions.

This system would be extensible, based on open standards such as REST or CoAP, [8][13] and could easily fit into a larger ‘smart home for the disabled’ or internet-of-things system.

## B.3 Method

Achieving these aims involves performing research and development in several discrete phases.

### B.3.1 Hardware

A list of possible sensor candidates will be developed, and these candidates will be ranked according to their adherence to the four accessibility criteria outlined above. Primarily the sensor ranking will consider the cost, invasiveness and reliability of detection, as the sensors themselves do not form a large part of the power requirement.

Similarly, a list of possible embedded boards to act as the sensor’s host and data analysis platform will be created. Primarily, they will be ranked on cost, energy efficiency and reliability of programming/system stability.

Low-powered wireless protocols will also be investigated, to determine which is most suitable for the device; providing enough range at low power consumption to allow easy and reliable communication with the hardware.

Once promising candidates have been identified, components will be purchased and analysed to determine how well they can integrate.

### B.3.2 Classification

Depending on the final sensor choice, relevant experiments will be performed to determine the classification algorithm with the best occupancy determina-

tion accuracy. This will involve the deployment of a prototype to perform data gathering, as well as another device/person to assess ground truth.

### B.3.3 Robustness / API

Once the classification algorithm and hardware are finalised, an easy to use API will be developed to allow the data the device collects to be integrated into a broader system.

The finalised product will be architected into a easy-to-install software solution that will allow someone without domain knowledge to use the software and corresponding hardware in their own environment.

## B.4 Timeline

Date	Task
Fri 15 August	<i>Project proposal and project summary due to Coordinator</i>
August	Hardware shortlisting / testing
25–29 August	<i>Project proposal talk presented to research group</i>
September	Literature review
Fri 19 September	<i>Draft literature review due to supervisor(s)</i>
October - November	Core Hardware / Software development
Fri 24 October	<i>Literature Review and Revised Project Proposal due to Coordinator</i>
November - February	<i>End of year break</i>
February	Write dissertation
Thu 16 April	<i>Draft dissertation due to supervisor</i>
April - May	Improve robustness and API
Thu 30 April	<i>Draft dissertation available for collection from supervisor</i>
Fri 8 May	<i>Seminar title and abstract due to Coordinator</i>
Mon 25 May	<i>Final dissertation due to Coordinator</i>
25–29 May	<i>Seminar Presented to Seminar Marking Panel</i>
Thu 28 May	<i>Poster Due</i>
Mon 22 June	<i>Corrected Dissertation Due to Coordinator</i>

## B.5 Software and Hardware Requirements

A large part of this research project is determining the specific hardware and software that best fit the accessibility criteria. Because of this, an exhaustive list of software and hardware requirements are not given in this proposal.

A budget of up to \$300 has been allocated by my supervisor for project purchases. Some technologies with promise that will be investigated include;

**Raspberry Pi Model B+** Small form-factor Linux computer

Available from <http://arduino.cc/en/Guide/Introduction>; \$38

**Arduino Uno** Small form-factor microcontroller

Available from <http://arduino.cc/en/Main/arduinoBoardUno>; \$36

**Panasonic Grid-EYE** Infrared Array Sensor

Available from <http://www3.panasonic.biz/ac/e/control/sensor/infrared/grid-eye/index.jsp>; approx. \$33

**Passive Infrared Sensor**

Available from various places; \$10–\$20

## B.6 Proposal References

- [1] Ardunio. <http://arduino.cc/en/Guide/Introduction>. Accessed: 2014-08-09.
- [2] AUSTRALIAN BUREAU OF STATISTICS. Household water and energy use, Victoria: Heating and cooling. Tech. Rep. 4602.2, October 2011. Retrieved October 6, 2014 from <http://www.abs.gov.au/ausstats/abs@.nsf/0/85424ADCCF6E5AE9CA257A670013AF89>.
- [3] BALAJI, B., XU, J., NWOKAFOR, A., GUPTA, R., AND AGARWAL, Y. Sentinel: occupancy based HVAC actuation using existing WiFi infrastructure within commercial buildings. In *Proceedings of the 11th ACM Conference on Embedded Networked Sensor Systems* (2013), ACM, p. 17.
- [4] BELTRAN, A., ERICKSON, V. L., AND CERPA, A. E. ThermoSense: Occupancy thermal based sensing for HVAC control. In *Proceedings of the 5th ACM Workshop on Embedded Systems For Energy-Efficient Buildings* (2013), ACM, pp. 1–8.
- [5] CHAN, M., CAMPO, E., ESTÈVE, D., AND FOURNIOLS, J.-Y. Smart homes - current features and future perspectives. *Maturitas* 64, 2 (2009), 90–97.
- [6] ERICKSON, V. L., ACHLEITNER, S., AND CERPA, A. E. POEM: Power-efficient occupancy-based energy management system. In *Proceedings of the 12th international conference on Information processing in sensor networks* (2013), ACM, pp. 203–216.
- [7] ERICKSON, V. L., BELTRAN, A., WINKLER, D. A., ESFAHANI, N. P., LUSBY, J. R., AND CERPA, A. E. Demo abstract: ThermoSense: thermal array sensor networks in building management. In *Proceedings of the 11th ACM Conference on Embedded Networked Sensor Systems* (2013), ACM, p. 87.
- [8] GUINARD, D., ION, I., AND MAYER, S. In search of an internet of things service architecture: REST or WS-\*? a developers perspective. In *Mobile and Ubiquitous Systems: Computing, Networking, and Services*. Springer, 2012, pp. 326–337.

- [9] HAILEMARIAM, E., GOLDSTEIN, R., ATTAR, R., AND KHAN, A. Real-time occupancy detection using decision trees with multiple sensor types. In *Proceedings of the 2011 Symposium on Simulation for Architecture and Urban Design* (2011), Society for Computer Simulation International, pp. 141–148.
- [10] HNAT, T. W., GRIFFITHS, E., DAWSON, R., AND WHITEHOUSE, K. Doorjamb: unobtrusive room-level tracking of people in homes using doorway sensors. In *Proceedings of the 10th ACM Conference on Embedded Network Sensor Systems* (2012), ACM, pp. 309–322.
- [11] KLEIMINGER, W., BECKEL, C., DEY, A., AND SANTINI, S. Poster abstract: Using unlabeled Wi-Fi scan data to discover occupancy patterns of private households. In *Proceedings of the 11th ACM Conference on Embedded Networked Sensor Systems* (2013), ACM, p. 47.
- [12] KLEIMINGER, W., BECKEL, C., STAACE, T., AND SANTINI, S. Occupancy detection from electricity consumption data. In *Proceedings of the 5th ACM Workshop on Embedded Systems For Energy-Efficient Buildings* (2013), ACM, pp. 1–8.
- [13] KOVATSCH, M. CoAP for the web of things: from tiny resource-constrained devices to the web browser. In *Proceedings of the 2013 ACM conference on Pervasive and ubiquitous computing adjunct publication* (2013), ACM, pp. 1495–1504.
- [14] Raspberry pi. <http://www.raspberrypi.org/>. Accessed: 2014-08-09.
- [15] TING, K., YU, R., AND SRIVASTAVA, M. Poster Abstract: Occupancy inferencing from non-intrusive data sources. In *Proceedings of the 5th ACM Workshop on Embedded Systems For Energy-Efficient Buildings* (2013), ACM, pp. 1–2.
- [16] YANG, Z., LI, N., BECERIK-GERBER, B., AND OROSZ, M. A multi-sensor based occupancy estimation model for supporting demand driven HVAC operations. In *Proceedings of the 2012 Symposium on Simulation for Architecture and Urban Design* (2012), Society for Computer Simulation International, p. 2.